Dihydrogen Bonding: Structures, Energetics, and Dynamics

Radu Custelcean*,† and James E. Jackson*

Department of Chemistry, Michigan State University, East Lansing, Michigan 48824

Received September 5, 2000

Contents

I. Introduction

Hydrogen bonding occupies a prominent position in modern chemistry.[1] It is fundamental for molecular recognition and supramolecular synthesis and holds a central role in biology.[2] Typically, this interaction occurs between the positively charged hydrogen of an A−H (A = O, N, halogen, C) proton donor and the lone pair of an electronegative element, the π electrons of a multiple bond or aromatic ring, or a transition metal center, representing the proton acceptor.[3,4] Recently, an unusual type of hydrogen bonding, in which a σ M−H bond (where M is less electronegative than H) acts as the electron donor, has attracted considerable attention.[3−10]

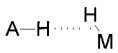

This hydridic-to-protonic interaction, also called dihydrogen bonding, proton-hydride bonding, H···H hydrogen bonding, or hydrogen−hydrogen bonding, has strength and directionality comparable with those found in conventional hydrogen bonding. Consequently, it can influence structure, reactivity, and selectivity in solution and solid state, finding thus potential utilities in catalysis, crystal engineering, and materials chemistry.

* To whom correspondence should be addressed.
† Current Address: Department of Chemical Engineering and Materials Science, University of Minnesota, Minneapolis, MN 55455.

Radu Custelcean was born in 1972 in Romania and earned his B.S. and M.S. degrees in Chemistry from Babes-Bolyai University, Romania, in 1995 and 1996, respectively. He then moved to Michigan State University where he received his Ph.D. in Chemistry under the guidance of Professor James E. Jackson, in 2000. Currently he is a postdoctoral associate in the group of Professor Michael D. Ward at the University of Minnesota. His research interests include self-assembly and supramolecular synthesis using hydrogen bonds, structure and reactivity of organic molecular crystals, and organic inclusion compounds.

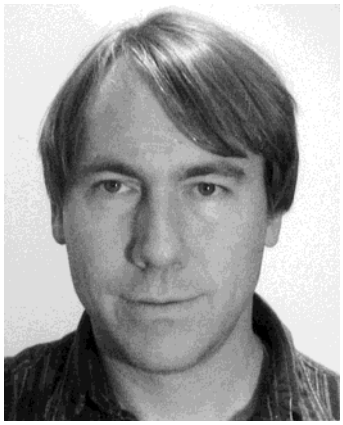

Ned Jackson was born in 1955 in Boston, Massachusetts. After obtaining his A.B. from Harvard in 1977 (Bill Gates's class!), he sailed twice across the Atlantic, flirted with Oceanography research in a NOAA lab, and after starting graduate study with Wes Borden at the University of Washington, moved to Princeton where he earned his Ph.D. in Chemistry under the guidance of Professors Maitland Jones, Jr., and Leland C. Allen, in 1987. After a wonderful postdoctoral stay with Matt Platz at Ohio State University, he joined the Chemistry faculty at Michigan State University. His research interests include experimental and computational studies of reactive intermediates, design of organic molecular magnetic materials, development of biomass-based catalytic pathways to "petrochemicals", and of course, dihydrogen bonding.

This review summarizes the emergence and development of this topic, starting with the early observations of H···H bonding, continuing with its compre-

10.1021/cr000021b CCC: $36.00
Published on Web 05/19/2001

hensive structural and energetic description, and concluding with the implications of this interaction in supramolecular synthesis, as well as its influence on reactivity and selectivity in both solution and the solid state. While short accounts describing advances in particular aspects of this area have been previously published,[3−10] the purpose of this paper is to provide a comprehensive picture of dihydrogen bonding, unifying all reports available to date around the common themes of structure, energetics, and dynamics.

II. Structural and Energetic Characterization

A. Dihydrogen Bonding to the Main Group Hydrides

Chemists had intuitively thought about proton−hydride interactions long before these associations were formally categorized as hydrogen bonds. In 1934, Zachariasen and Mooney reported the crystal structure of ammonium hypophosphite ($NH_4^+H_2PO_2^-$)[11] and noted that "the hydrogen atoms of the hypophosphite group behave toward ammonium as if they were H^- ions".[12] Thirty years later, Burg suggested the presence of N−H···H_3B interactions comparable to hydrogen bonds in liquid $(CH_3)_2NH\cdot BH_3$, based on the perturbation of the N−H and B−H bands in the IR spectrum.[13] Titov et al. explained the enhanced chemical reactivity of aminoboranes toward H_2 loss by the "close spatial arrangement of the oppositely charged hydrogen atoms".[14]

However, the first to recognize this interaction as a true hydrogen bond were M. P. Brown and co-workers in the late 1960s.[15,16] On the basis of a thorough analysis of the IR spectra of the boron coordination compounds $L\cdot BH_3$ (L = Me_3N, Et_3N, Py, Et_3P) and $Me_3N\cdot BH_2X$ (X = Cl, Br, I) in the presence of proton donors such as MeOH, PhOH, and *p*-F-C_6H_4-OH in CCl_4, they proposed the formation of a novel type of hydrogen bond in which the BH_3 and BH_2 groups acted as proton acceptors, despite their lack of lone pairs or π electrons. They measured the strengths of these interactions by variable temperature IR spectroscopy, finding association energies in the range of 1.7−3.5 kcal/mol, comparable with moderately strong conventional hydrogen bonds.[17] Similarly, they inferred the occurrence of intermolecular NH···H_3B hydrogen bonding in $Me_2NH\cdot BH_3$ and $(RNH\cdot BH_2)_3$ (R = Pr, Bu) from the temperature- and concentration-dependence of these compounds' N−H stretching absorptions in CCl_4.[15,16]

In a recent study, Epstein and co-workers confirmed the ability of boron hydrides to act as proton acceptors in hydrogen bonds.[18−20] They studied the interaction of neutral NEt_3BH_3 and $P(OEt)_3BH_3$ as well as ionic $Bu_4N^+BH_4^-$ with different alcohols as proton donors, by IR and NMR spectroscopy in CH_2Cl_2, C_6H_{14}, and C_6D_{12}, and concluded that the properties of these unconventional OH···HB interactions are similar to those found in classical hydrogen bonds. Their association energies were found to increase proportionally with the proton donors' acidities, being situated in the range 1.1−3.7 and 2.3−6.5 kcal/mol, for the neutral and ionic boron hydrides, respectively. Theoretical calculations (RHF/6-31G) confirmed the attractive nature of these proton−hydride interactions.

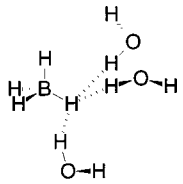

Figure 1. O-H···H−B dihydrogen bonds found in $NaBH_4\cdot 2H_2O$ in the solid state.

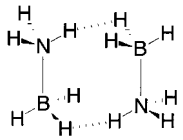

Figure 2. C_2 isomer of the NH_3BH_3 dimer.

The solution studies, however, cannot unambiguously establish whether these unusual interactions involve the boron atom, the hydridic hydrogen, or the BH group as a whole. We have recently determined the X-ray and neutron crystal structures of $NaBH_4\cdot 2H_2O$ and $NaBD_4\cdot 2D_2O$ to probe the existence of O−H···H−B dihydrogen bonding in the solid state and provide a detailed structural description of it.[21] We found three close H···H contacts of 1.79, 1.86, and 1.94 Å, respectively (Figure 1), substantially shorter than the 2.4 Å distance corresponding to twice the van der Waals radius of a hydrogen atom. The O−H vectors clearly point toward the middle of the B−H bonds, suggesting association with the σ-bond electrons, rather than B or H atoms.

The same conclusion can be drawn from the systematic Cambridge Structural Database (CSD) search done by Crabtree et al. for boron−nitrogen compounds.[22] The 26 intermolecular N−H···H−B short contacts found in the range 1.7−2.2 Å, for which Crabtree suggested the term "dihydrogen bonds", showed a strong preference for a bent geometry, with NH···H−B angles typically situated between 95 and 120°, and N−H···HB angles tending to be larger (150−170° in most of the cases). These side-on structures were rationalized in terms of negative charges on both B and H atoms, with the bending allowing the protonic NH to approach the partially negative B atom, thus maximizing the attractive electrostatic interaction. They also investigated theoretically the NH_3BH_3 dimer, whose C_2 symmetrical geometry (Figure 2) optimized at the PCI-80/B3LYP level of theory showed two identical H···H interactions, with contact distances of 1.82 Å and NH···H−B and N−H···HB angles of 98.8 and 158.7°, respectively, falling in the range found by the CSD search. The calculated dimerization energy of −12.1 kcal/mol corresponds to 6.1 kcal/mol per N−H···H−B interaction, which, as suggested by Crabtree, could account for the strikingly higher melting point of aminoborane (+104 °C) relative to the isoelectronic ethane (mp −181 °C).[22]

A similar head-to-tail arrangement was also found by Cramer and Gladfelter in their theoretical study

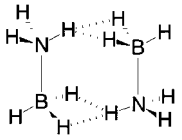

Figure 3. C_{2h} isomer of the NH_3BH_3 dimer.

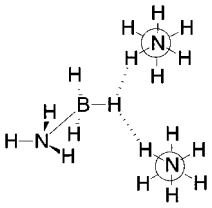

Figure 4. The shortest N−H···H−B contacts found in NH_3BH_3 in the solid state.

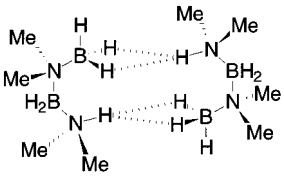

Figure 5. Dihydrogen-bonded dimers found in $(CH_3)_2NH-BH_2-N(CH_3)_2-BH_3$ in the solid state.

of the $(NH_3BH_3)_2$ dimer.[23] However, using HF, DFT, or MP2 methods, they found a C_{2h} symmetrical structure as the global minimum (Figure 3), which lies only 0.2 kcal/mol lower in energy than the C_2 isomer reported by Crabtree et al. This geometry allows the formation of bifurcated dihydrogen bonds with H−H distances of 1.990 Å, and NH···H−B and N−H···HB angles of 88.6 and 144.8°, respectively, as calculated at the MP2/cc-pVDZ level. The association energy obtained at the same level of theory is −15.1 kcal/mol.

For comparison, the crystal structure of NH_3BH_3 recently determined by Crabtree and co-workers by neutron diffraction shows a packing that results in three short intermolecular N−H···H−B interactions, with the shortest one exhibiting a H−H distance of 2.02 Å and values for the NH···H−B and N−H···HB angles of 106(1) and 156(3)°, respectively (Figure 4).[24] Again, the N−H vectors point toward the middle of the B−H bonds, suggesting that the σ-bond as a whole represents in fact the proton acceptor partner in these interactions.

Further insight into the nature of the N−H···H−B interaction was provided by Popelier, who applied the "atoms in molecules" theory on the same $(NH_3BH_3)_2$ dimer and concluded that this interaction can indeed be classified as a hydrogen bond.[25]

Intermolecular N−H···H−B interactions have also been described by Nöth et al., who recently reported the crystal structure of $(CH_3)_2NH-BH_2-N(CH_3)_2-BH_3$, which self-assembles into dihydrogen-bonded dimers, as illustrated in Figure 5.[26]

The N−H···H−B dihydrogen bonding can also form intramolecularly, as found in the crystal structure of the 2′-deoxycytidine-*N*(3)-cyanoborane (**1**), which shows a close H···H contact of 2.05 Å.[27,28]

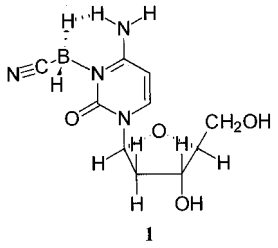

1

Intramolecular C−H···H−B close contacts are present in the aminoboron hydrides **2**−**6**, which could be responsible for the stabilization against disproportionation in these complexes.[29]

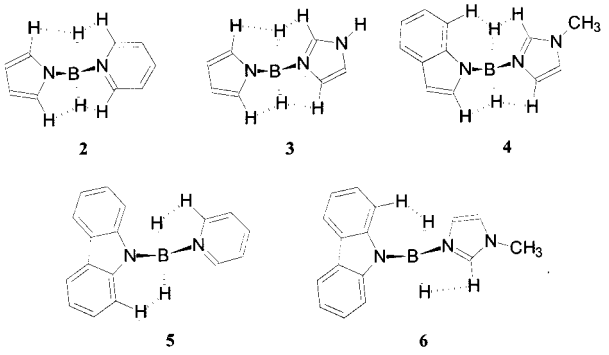

2 **3** **4** **5** **6**

Their X-ray crystal structures show multiple H−H distances below 2.65 Å, which was considered the threshold intermolecular distance for H···H interactions in this study.[30] The heterocyclic rings adopt almost coplanar orientations relative to the B−H bonds, maximizing thus the intramolecular H···H associations. The relatively small H−C−N exocyclic angles next to the B−H bonds in some of these complexes, as compared to the free heterocycles, also suggest attractive interactions between the protonic hydrogens on the α-carbons and the hydridic BH hydrogens. In solution, the formation of similar dihydrogen bonds was explored by NOE experiments. For instance, **2** adopts a conformation comparable to the one found in the solid state, allowing again short C−H···H−B contacts. It is intriguing, however, that in the gas phase the two rings prefer an orthogonal orientation, as indicated by HF/6-31G* calculations.

Intramolecular C−H···H−B dihydrogen bonds were also proposed to play an important role in controlling the conformation of the azacyclohexane−borane adducts **7**−**10**.[31]

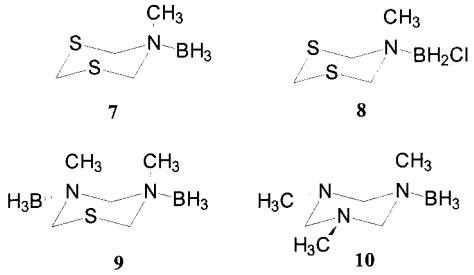

7 **8** **9** **10**

Thus, the BH_3 groups are always found in the equatorial position in these complexes, which appears to be the result of favorable attractive interactions between the hydridic B−H hydrogens and the positively charged H atoms of the α-CH_2 groups (Figure 6). Associations with the C−H hydrogens of the N−CH_3 group also seem to stabilize these structures,

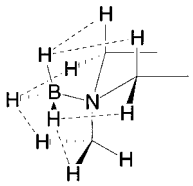

Figure 6. C−H···H−B close contacts in **7**−**10**.

as indicated by the short H−H distances and the decrease of the $H_3C-N-BH_3$ angles relative to the $H_3C-N-CH_3$ angle in the $(CH_3)_2N^+$ derivative.

The hydrides of the heavier group 3 elements are also capable of forming dihydrogen bonds. Thus, in 1994, Raston and co-workers provided X-ray crystallographic evidence for an intramolecular N−H···H−Al interaction in the alane-piperidine adduct **11**.[32] The H−Al−N−H unit has an eclipsed conformation in the solid state, allowing the two oppositely charged hydrogen atoms to approach to 2.31 Å, in direct contrast to the previously reported structures of aminoalanes, which are known to exhibit a staggered conformation about the Al−N bond. This arrangement, Raston noted, represents an intermediate prior to H_2 evolution, to form an amidometal species.

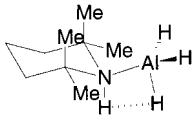

11

Computational studies at the MP2/cc-pVDZ level, by Cramer and Gladfelter,[23] revealed a staggered C_{3v} symmetrical geometry for NH_3AlH_3, which upon dimerization forms a C_2 symmetrical structure (Figure 7) that contains two short intermolecular N−H···H−Al hydrogen bonds, with an H−H separation of 1.781 Å, and NH···H−Al and N−H···HAl angles of 119.4 and 172.0°, respectively. The dimerization energy calculated at the same level of theory is −11.8 kcal/mol, which corresponds to about 6 kcal/mol per N−H···H−Al dihydrogen bond.

Cyclotrialumazane ($(NH_2AlH_2)_3$) was found theoretically (MP2/cc-pVDZ) to prefer the twist-boat over the chair conformation in the gas phase, by as much as 2.8 kcal/mol, due to favorable electrostatic $N-H^{\delta+}-{}^{\delta-}H-Al$ flagpole interactions (Figure 8).[33] In the solid state, however, it is likely that it will adopt the chair arrangement for a more efficient packing, as also observed in the analogous boron and gallium sys-

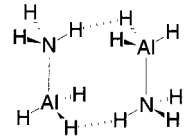

Figure 7. Calculated structure of the NH_3AlH_3 dimer.

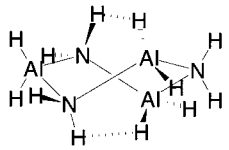

Figure 8. Calculated structure of $(NH_2AlH_2)_3$.

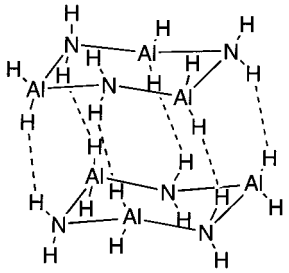

Figure 9. Calculated structure of the $(NH_2AlH_2)_3$ dimer.

tems. On the basis of this consideration, the chair conformer was used for the calculation (RHF/cc-pVDZ) of the preferred geometry in the $[(NH_2AlH_2)_3]_2$ dimer. As shown in Figure 9, the resulting C_{3v} symmetrical structure exhibits six short H−H contacts, and the enthalpy of dimerization is predicted to be −9.9 kcal/mol at the MP2/cc-pVDZ//RHF/cc-pVDZ level.

The next element in group 3, gallium, can also be involved in dihydrogen bonding, as Gladfelter's neutron diffraction crystal structure of cyclotrigallazane (**12**) demonstrates.[33]

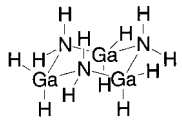

12

In the solid state, **12** forms an α-network, by participating in four N−H···H−Ga intermolecular interactions, with H−H distances of 1.97 Å (Figure 10). The observed NH···H−Ga and N−H···HGa angles are rather close, with values of 131 and 145°, respectively. The strength of these dihydrogen bonds was estimated by theoretical calculations on the $[(NH_2GaH_2)_3]_2$ dimer. As in the aluminum analogue, the monomer prefers the twist-boat conformation by 2.6 kcal/mol, favoring thus intramolecular H···H interactions involving the oppositely charged H atoms from the flagpole positions. However, for direct comparison with the solid-state structure, the chair conformation was considered for the geometry optimization of the dimer. The highest dimerization energy was found for the C_s symmetrical structure illustrated in Figure 11, from which an interaction energy of about 3 kcal/mol could be estimated for each N−H···H−Ga dihydrogen bond. In the case of the $(NH_3GaH_3)_2$ dimer, theoretical calculations by Cramer and Gladfelter predicted a C_2 symmetrical geometry similar to the one found in the Al analogue, with

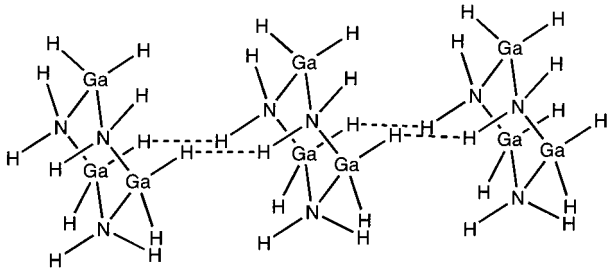

Figure 10. Self-assembly of cyclotrigallazane in the solid state.

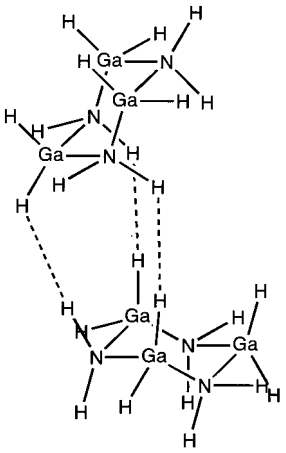

Figure 11. Calculated structure of the $(NH_2GaH_2)_3$ dimer.

N−H···H−Ga dihydrogen bonds of approximately 5 kcal/mol in strength.[23]

Formation of dihydrogen-bonded complexes by other main group hydrides such as LiH, BeH_2, or the recently discovered XeH_2, has been investigated theoretically by a number of researchers.[34−39] A theoretical study (MP2 and B3LYP) of the dihydrogen-bonded complexes between the hydrides LiH, NaH, BeH_2, MgH_2, CH_4, SiH_4, GeH_4, SnH_4, and hydrofluoric acid, reported by Grabowski, demonstrated the existence of direct correlations between H···H distances and H-bonding energies.[40] Also, the H···H separations have been found to be inversely proportional to the F−H bond lengths, as is seen in conventional O−H···O or N−H···O hydrogen bonds.[40,41]

B. Dihydrogen Bonding to Transition Metal Hydrides

In 1986, Milstein and co-workers reported the X-ray crystal structure of the iridium hydride complex **13**, in which they noted an unusually small Ir−O−H angle of 91° and an eclipsed H−Ir−O−H conformation, indicating an attractive H···H interaction.[42] However, the H−H distance of 2.441 Å was too long for a hydrogen bond. The later neutron diffraction study of the same compound revealed a shorter H−H distance of 2.40 Å, but a wider Ir−O−H angle of 104.4°.[43]

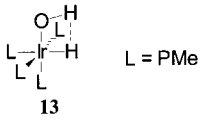

13

In 1994, Berke and collaborators suggested that the formation of $M-H^{\delta-}\cdots H^{\delta+}-X$ interactions might precede the protonation of transition metal hydrides to yield dihydrogen complexes (Scheme 1).[44]

The first unequivocal evidence of dihydrogen bonding involving a transition metal hydride came independently from the groups of Crabtree and Morris in 1994. The X-ray crystal structure of **14** determined by Crabtree et al. showed an unexpected tautomerization of the amide group from the ligand into the iminol form, facilitating thus the interaction between the hydridic Ir−H and the OH proton.[45]

Scheme 1

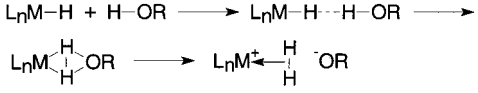

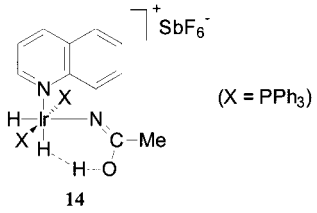

14

While the exact H−H distance could not be determined in the solid state due to the failure to locate the Ir−H hydrogen, ^{1}H NMR T_1 relaxation time measurements in solution gave a H···H contact distance of about 1.8 Å. The interaction seems to have some covalent character, as demonstrated by the observed coupling of 3 Hz between Ir−H and O−H hydrogens.

An even higher coupling of 5.5−5.6 Hz was found in **15** (Y = H, Cl, Br, I), in which the H···H contact distance was estimated at around 1.7 Å (Y = Cl), based on T_1 relaxation time measurements.[46]

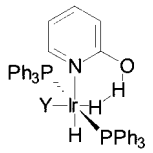

15

These H···H interactions are fairly strong, competing favorably with the conventional Y···H hydrogen bonds, as demonstrated by the predominance of the O−H···H−Ir dihydrogen-bonded rotamers over the opposite O−H···Y−Ir hydrogen-bonded ones.

A quantitative estimation of the strength of these unconventional hydrogen bonds involving iridium hydride complexes was elegantly made by Crabtree's group in the analogous 2-aminopyridine complexes **16** (Y = H, F, Cl, Br, I, CN, CO).[46] They measured the rotation barrier for the NH_2 group, which represents the sum of the H···H interaction energy and the intrinsic rotation barrier around the C−N bond in the ligand. The strongest N−H···H−Ir hydrogen bond (5.0 kcal/mol) was found for the case where Y = H, while the trans Y ligand tends to weaken the interaction in the order: F > Cl > Br > I > CN > CO > H, which can be rationalized by their decreasing electronegativity in the same order.

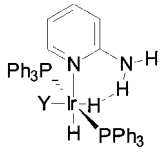

16

Morris and co-workers demonstrated the presence of H···H interactions in the iridium hydride complex **17** by X-ray diffraction in the solid-state and NMR spectroscopy in solution.[47]

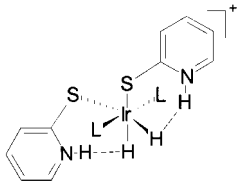

17 (L = PCy_3)

18 (L = PH_3)

The crystal structure of **17** indicated a close contact between the pyridinium protons and the Ir−H hydridic hydrogens, which unfortunately could not be located precisely from the electron density difference maps. Nevertheless, their ^{1}H NMR data provided clear evidence for N−H···H−Ir hydrogen bonding in CD_2Cl_2, with a H−H contact distance of about 1.75 Å, calculated from the observed T_1 relaxation times of the protonic and hydridic hydrogens. Theoretical calculations by Hoffmann et al.[34] on the model complex **18** confirmed the attractive H···H interaction and concluded that its nature is mostly electrostatic. Interestingly, when THF was used as a solvent, the dihydrogen bonds were switched off in **17**, presumably due to the formation of conventional N−H···O hydrogen bonds with the solvent.[47]

Bifurcated N−H···H(Ir)···H−N dihydrogen bonds were also detected by Morris et al. in **19** and **20** by X-ray crystallography and NMR spectroscopy, and their H−H contact distances were estimated around 1.80 and 1.86 Å, respectively, in solution.[48]

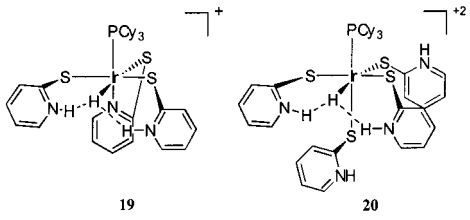

19 **20**

The same group also reported an interesting bifurcated Ir−H···H(N)···F−B interaction in complex **21**, in which the N−H proton is shared by a hydridic Ir−H hydrogen and a conventional B−F electron donor from the BF_4^- counterion.[49]

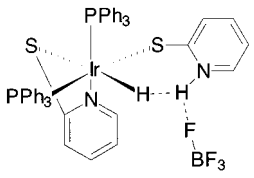

21

The occurrence of intermolecular X−H···H−M dihydrogen bonds was first documented by Crabtree and his collaborators, with the neutron diffraction crystal structure of the rhenium polyhydride complex **22**, which exhibits a three-center interaction between two Re−H hydrides and the N−H proton from an indole molecule of crystallization.[50−52] The geometrical parameters for the two H···H contacts, i.e., H−H distances of 1.73 and 2.21 Å, and strongly bent NH···H−Re angles of 119 and 97°, respectively, fall in the range expected for dihydrogen bonding. The strength of the interaction was estimated around 4.3 kcal/mol, from the shift of the N−H stretching band in the solid-state IR spectrum of **22**, relative to free indole.

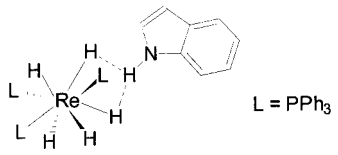

22

Theoretical calculations using the DFT method on a $[ReH_5(PH_3)_3]\cdot NH_3$ model confirmed the attractive nature of the interaction and predicted a similar three-center hydrogen bond with H···H distances of 1.92 and 2.48 Å, and an interaction energy of 8 kcal/mol in the gas phase.

The intermolecular N−H···H−Re hydrogen bonding appears to be general, as demonstrated by the X-ray crystal structure of the analogous complex **23**, in which the role of the proton donor is played by an imidazole molecule.[51,53] The H−H distances could not be satisfactorily determined due to the failure to locate the N−H hydrogen from the disordered imidazole. The strength of the interaction (5.3 kcal/mol, estimated by IR spectroscopy) is greater than in the similar complex **22**, as expected considering the higher acidity of imidazole relative to indole.

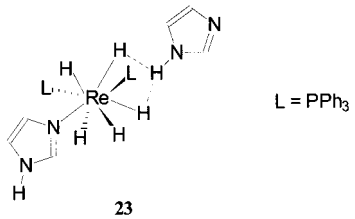

23

Other weak acids such as 2,4,6-$Me_3C_6H_2OH$, 2-*t*Bu-6-MeC_6H_3OH, pyrrole, PhNHPh, PhNHBn, and PhNHMe, also associate with $ReH_5(PPh_3)_2$, as shown by the IR spectra of the thin films obtained by evaporation of CH_2Cl_2 solutions containing a 1:1 mixture of the polyhydride and the proton donor.[54] The $-\Delta H^0$ of the interactions, evaluated from the observed shifts of the NH or OH bands, were found to generally correlate with the acidities of the proton donors and vary between 3.0 and 5.8 kcal/mol. Replacing the hydridic partner with the $WH_4(PMePh_2)_4$ complex resulted in slightly weaker dihydrogen bonds of 1.1−5.2 kcal/mol. That these interactions involve primarily the hydridic hydrogen and not the d^2 nonbonding electron pairs of the Re or W metals was demonstrated by the analogous d^0 complex ReH_7(dppe) (dppe = $Ph_2PCH_2CH_2PPh_2$), that also associated with the same proton donors, with $-\Delta H^0$ in the range 1.3−4.7 kcal/mol.

In solution, the N−H···H−Re interactions were studied by Crabtree et al. using UV−vis spectroscopy.[55] Thus, the $ReH_5(PPh_3)_2L$ (L = pyridine, 4-picoline, 4-(dimethylamino)pyridine, and 4-carbomethoxypyridine) hydrogen bond acceptors interact with indole, as the hydrogen bond donor, showing free energies of association, $-\Delta G$, of 3.8−5.0 kcal/mol.

In a thorough analysis, Epstein, Berke, and coworkers surveyed dihydrogen bonding in solution in the tungsten hydride-alcohol complexes **24** (ROH =

phenol, hexafluoro-2-propanol (HFIP), and perfluoro-2-methyl-2-propanol (PFTB)).[56]

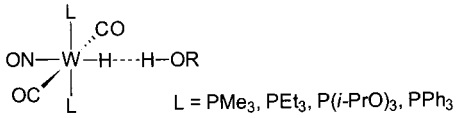

24

Using IR and NMR spectroscopies, they ruled out hydrogen bonding to the CO or NO groups and proved the exclusive formation of the unconventional O−H···H−W interactions. As expected, the strengths of these dihydrogen bonds increase with the donor abilities of the ligand L (PMe_3 > PEt_3 > $P(Oi\text{-}Pr)_3$ > PPh_3) and are directly proportional to the acidities of the proton donors (PFTB > HFIP > PhOH). Their association energies fall in the estimated range 4.1−6.9 kcal/mol, based on both the observed shifts in the corresponding ν_{OH} bands, and the variation of the association constants K with temperature. In addition, NMR experiments (δ shifts, NOE, and T_1 relaxation times) all supported the formation of O−H···H−W dihydrogen bonds, with H−H contact distances as short as 1.77 Å, as observed in the case of HFIP. A linear OH···H−W orientation was arguably suggested for these interactions, in sharp contrast to the previously established propensity of dihydrogen bonds for a strongly bent geometry.

In an analogous series of rhenium hydride complexes (**25**), the same two research groups proved the occurrence of intermolecular O−H···H−Re dihydrogen bonding in solution.[57,58]

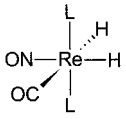

25

L = PMe_3 (**a**), PEt_3 (**b**), $Pi\text{-}Pr_3$ (**c**)

When PFTB was used as proton donor, interaction energies between 4.5 and 6.1 kcal/mol were calculated from the observed ν_{OH} shifts in the IR spectra in hexane. In toluene, however, the ΔH values, derived from variable temperature NMR spectroscopy, are smaller by about 3 kcal/mol, apparently due to competitive O−H···π interactions with the solvent.[58] The H···H contact distances calculated from T_1 relaxation times range between 1.78 and 1.94 Å. The phosphine ligand appears to have an important influence over the regioselectivity of the H-bonding formation. Thus, in **25a** interaction with one of the hydridic hydrogens is preferred, but the NO group competes more and more effectively for the proton donor as the bulkiness of L increases, to the point where only O−H···ON hydrogen bonds are observed for **25c**. DFT calculations on a $ReH_2(CO)(NO)(PH_3)_2 \cdot H_2O$ model indicated that the H···H interaction is energetically preferred by about 3.0−3.5 kcal/mol.[57] Also, a stronger interaction is predicted with the Re−H hydride trans to the NO group (d_{H-H} = 1.49 Å) as compared to the Re−H trans to CO (d_{H-H} = 1.79 Å) and confirmed experimentally by the high regioselectivity displayed by both PFTB and HFIP alcohols toward the former, as shown by NMR spectroscopy.

The experimental results obtained by Epstein and Berke on the intermolecular dihydrogen bonding in solution were complemented by the theoretical work by Scheiner et al. on the Mo and W hydride complexes **26**.[59] Their HF/3-21G and DFT (B3LYP, BLYP, B3PW91) calculations confirmed that the H···H interactions are favored over conventional hydrogen bonding involving the NO group.

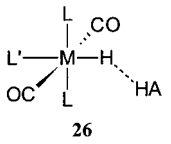

M = Mo, W
L = PH_3, NH_3
L' = NO, Cl, H
A = F, OH, H_2O^+

26

The dihydrogen bonds in **26** become stronger and shorter with the increases in the donating ability of the *cis*-ligand or the acidity of the proton donor, consistent with experiment. However, the strongly acidic H_3O^+ induces complete proton transfer, resulting in the formation of an η^2-H_2 dihydrogen complex. The H−H−M angles are strongly bent in all the optimized structures, as illustrated in Figure 12 for the representative complex **26a**. For this dihydrogen-bonded system, a 2.6 kcal/mol destabilization energy was calculated for a linear F−H···H−Mo orientation.

As seen with the boron hydrides, C−H sites may interact as the protonic partners with transition metal hydrides. Recent X-ray structural studies and CSD surveys confirmed the existence of intra-[60−63] as well as intermolecular[64] C−H···H−M close contacts in transition metal hydride complexes. A large number of these examples were observed in complexes containing $R_{3-x}(Ph)_xP$ (x = 1−3) ligands, in which one or more *ortho* C−H bonds point toward the M−H hydridic hydrogens (Figure 13).

While the H···H distances and M−H···H angles in these complexes were found to fall essentially in the same range as observed for the more "conventional" dihydrogen bonds involving N−H or O−H proton donors, the C−H···H angles usually tend to be smaller, due to the inherent constraints imposed by the chelation.[60] Caution is advisable in interpreting some of these C−H···H−M short contacts, however,

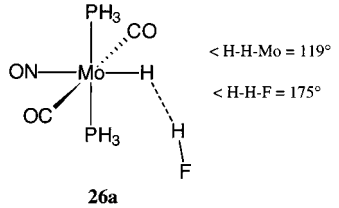

26a

Figure 12. Calculated structure for dihydrogen-bonded complex **26a**.

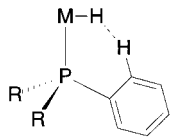

Figure 13. Generic representation of C−H···H−M dihydrogen bonds in complexes of transition metal hydrides with $R_{3-x}(Ph)_xP$ ligands.

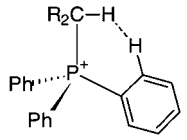

Figure 14. Generic representation of non-dihydrogen-bonded structures displaying short H···H contacts, in compounds containing the PPh_3 group.

as steric compression by bulky ligands or packing forces may make a significant contribution to the observed H···H close proximities.[61] For instance, a CSD survey of analogous structures that lack hydridic hydrogens (Figure 14) yielded 61 compounds displaying 89 Ph−H···H−C short contacts (<2.4 Å), of which 17 were below 2.2 Å![65] Thus, additional evidence is needed before close H···H contacts may be interpreted as attractive dihydrogen bonding interactions in such questionable cases.

The comprehensive analysis of the manganese hydride complex **27** carried out by Brammer and collaborators provided convincing evidence for an intramolecular C−H···H−Mn dihydrogen bond.[66] Their combined low-temperature neutron and X-ray diffraction study revealed a short intramolecular C−H···H−Mn contact of 2.10 Å, with H···H−Mn and C−H···H angles of 126.5 and 129.0°, respectively, and an essentially coplanar relative orientation of the Mn−H and C−H bonds (d Mn−H···H−C = 0.7°). The experimental atomic charges found for the Mn−H hydridic and *ortho* CH protonic hydrogens, of −0.40 and +0.32, clearly indicate an attractive electrostatic interaction, whose magnitude was calculated to be 5.7 kcal/mol. Moreover, topological analysis of the experimental charge density using the "atoms in molecules" theory unequivocally supported the existence of a moderately strong intramolecular C−H···H−Mn hydrogen bond.

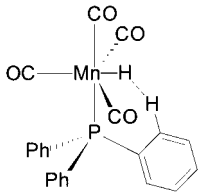

27

III. Self-Assembly of Extended Dihydrogen-Bonded Systems

In the previous section, it was demonstrated that dihydrogen bonding is a significant interaction, with energetic, electronic, and spectroscopic characteristics, as well as directionality, comparable with those found in conventional hydrogen bonding. A direct consequence of this similarity is that dihydrogen bonds, like traditional H-bonds, could find potential utility in crystal engineering and supramolecular synthesis. That these H···H noncovalent interactions are indeed capable of controlling crystal packing was already suggested by the crystal structure of cyclotrigallazane (**12**), which self-assembles into an extended dihydrogen-bonded α-network in the solid state (Figure 10), as demonstrated by Gladfelter's group.[33]

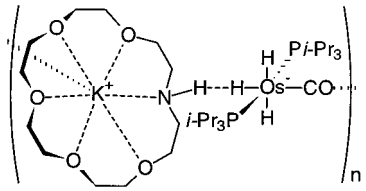

28

Figure 15. Self-assembly of dihydrogen-bonded complex **28** in one-dimensional chains.

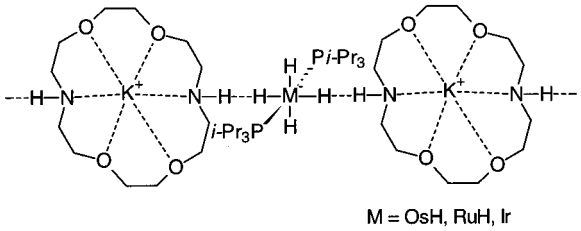

Figure 16. Self-assembly of dihydrogen-bonded complexes **29**·[K(1,10-diaza-18-crown-6)] in one-dimensional chains.

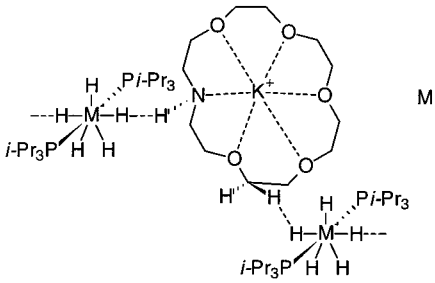

Figure 17. Self-assembly of dihydrogen-bonded complexes **29a,b**·[K(THF)(1-aza-18-crown-6)] in one-dimensional chains.

The osmium polyhydride complex [K(1-aza-18-crown-6)][*mer*-$OsH_3(CO)(i\text{-}Pr_3P)_2$] (**28**) synthesized by Morris et al. also forms polymeric one-dimensional chains in the solid-state (Figure 15).[67] The N−H···H−Os dihydrogen bonds are however complemented by CO···K^+ interactions in the assembly of the chains. When 1,10-diaza-18-crown-6 was used to complex K^+, similar chains held together exclusively by N−H···H−M dihydrogen bonds (Figure 16) could be assembled from the osmium, ruthenium, and iridium anionic polyhydrides $[MH_{x+3}(i\text{-}Pr_3P)_2]^-$ (M = Os (**a**), Ru (**b**), $x = 2$; M = Ir (**c**), $x = 1$) (**29**).[68,69] The intermolecular H···H distances in these complexes were estimated from their X-ray crystal structures to be in the range 1.8−1.9 Å. The NH bands in their solid-state IR spectra are broadened relative to the free diaza-crown ether and shifted to lower numbers by 96, 107, and 132 cm^{-1}, for the Os, Ru, and Ir complexes, respectively, in accord with the increasing basicity (and hydridic character) of these polyhydrides in the same order. The observed shifts correspond to N−H···H−M interaction energies of about 3 kcal/mol.[69]

Weaker C−H···H−M hydrogen bonds can also be involved in the supramolecular association of the polyhydrides **29a,b** with K(THF)(1-aza-18-crown-6), in which alternating NH···H−M−H···HN and CH···H−M−H···HC units lead to the formation of zigzag chains, as illustrated in Figure 17.[69] The NH···HOs and NH···HRu separations were estimated at 1.7 Å, while the weaker CH···HOs and CH···HRu

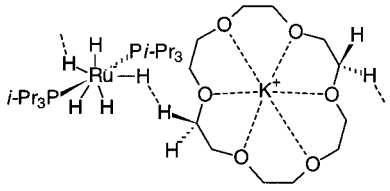

Figure 18. Self-assembly of dihydrogen-bonded complex **29b**·[K(THF)(18-crown-6)] in one-dimensional chains.

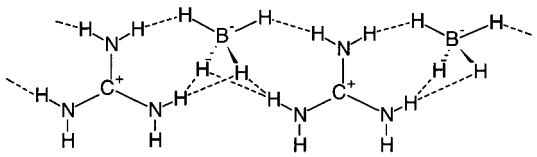

Figure 19. Self-assembly of guanidinium borohydride in one-dimensional extended tapes.

interactions exhibit longer H−H contact distances of 2.2 and 2.1 Å, respectively. Finally, a similar polymeric chain can be assembled exclusively by weak C−H···H−M interactions (Figure 18), as illustrated by the crystal structure of **29b**·[K(THF)(18-crown-6)].[69] In this case, the observed C−H···H−Ru contact distance is 2.2 Å.

As part of our own early endeavors directed toward the structural characterization of dihydrogen-bonded systems involving anionic borohydrides, we examined the crystal structure of guanidinium borohydride.[70] In the solid-state, this salt is organized into extended tapes, in which the alternating BH_4^- and $C(NH_2)_3^+$ ions are connected by multipoint dihydrogen bonds, as illustrated in Figure 19.

More recently, we have employed O−H···H−B dihydrogen bonds in the construction of one-, two-, and three-dimensional supramolecular networks self-assembled from various metal borohydrides and triethanolamine (TEA), in which the BH_4^- and M^+·TEA units represent the hydridic and protonic partners, respectively.[71,72]

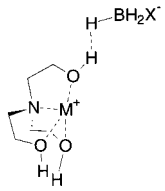

M = Li, X = H **30**
M = Na, X = H **31**
M = Na, X = CN **32**

Thus, in complex **30**, each Li^+ is pentacoordinated by the nitrogen and three oxygen atoms from a TEA molecule and by another oxygen atom from a different TEA molecule, forming $(Li^+TEA)_2$ dimers.[71] Multiple dihydrogen bonds link the dimers via BH_4^- pairs, giving rise to extended ribbons (Figure 20). A total of 10 different H···H short contacts are present, six from one BH_4^- and four from another, with H−H separations ranging between 1.69 and 2.32 Å. All hydrogen atoms were unambiguously located from the difference Fourier map, making these distances sufficiently reliable. The typical normalization of O−H and B−H bonds to 0.96 and 1.21 Å, respectively, leads to even shorter contact distances of 1.62−2.28 Å. The smallest two intermolecular dis-

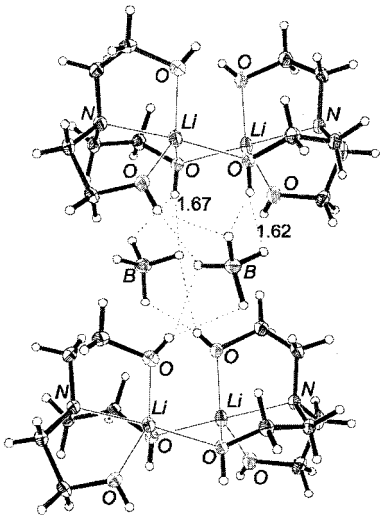

Figure 20. X-ray crystal structure of $LiBH_4$·TEA showing the H···H close contacts in Å. Reproduced with permission from ref 71. Copyright 1999 Wiley-VCH.

tances of 1.62 and 1.67 Å represent the shortest H···H contacts reported so far for dihydrogen bonds. They appear to be the result of the strong complexation of the OH groups by the Li^+ cations, which in turn increases the acidity of the corresponding protons. Notably, both OH groups involved in these two dihydrogen bonds contain bridging O atoms coordinating two Li^+ cations, which undoubtedly results in increased acidity of their corresponding protons and thus enhanced hydrogen bonding ability.

Figure 21 depicts the crystal structure of **31**.[72] In this case, one-dimensional $(Na^+TEA)_n$ coordination chains are formed, which are interconnected by O−H···H−B interactions into extended layers. Each BH_4^- interacts with two OH groups in one chain and one OH group from the next chain, with observed H−H contact distances ranging between 1.93 and 2.16 Å. These dihydrogen bonds appear to dominate the crystal packing of **31**, as no conventional hydrogen bonds are seen. Self-assembly into one-dimensional $(Na^+TEA)_n$ chains was also observed in **32**.[72] In this complex, the chains are further linked by O−H···H−B and CN···Na^+ interactions, into a three-dimensional extended network (Figure 22).

IV. Dynamics of Dihydrogen Bonds

Numerous studies have now established that dihydrogen bonding is an important and general interaction involving element−hydride σ bonds, and its geometrical and energetic features have been described in great detail. The significance of these unusual hydrogen bonds extends, however, beyond their fundamental aspects. With their substantial strength and directionality they can be used to control reactivity and selectivity of chemical reactions, at the same time finding a place alongside conventional hydrogen bonding in the supramolecular chemists' arsenal of noncovalent interactions. However, what makes dihydrogen bonding particularly interesting is the special reactivity conferred by its peculiar nature. It has been recently demon-

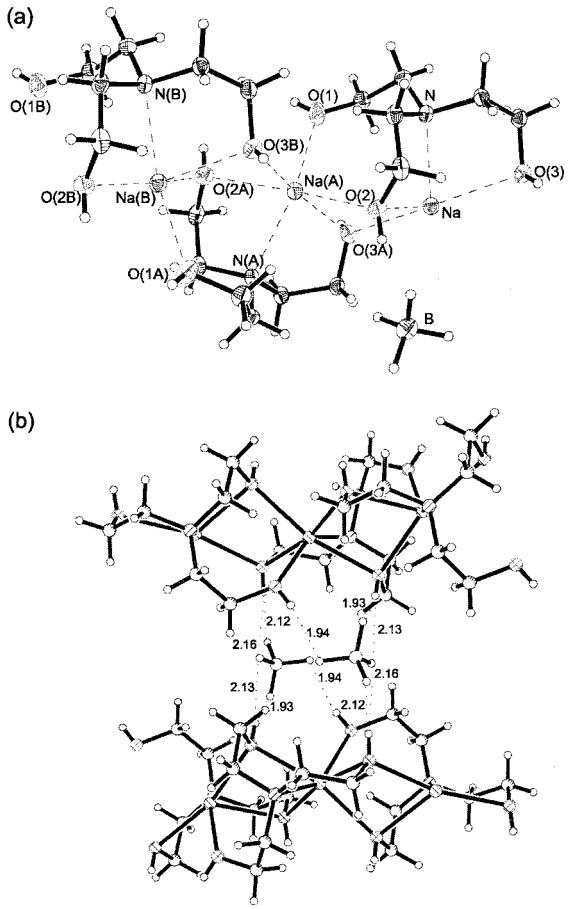

Figure 21. X-ray crystal structure of $NaBH_4$·TEA: (a) coordination of Na^+; (b) dihydrogen bonds connecting the chains, with H−H contact distances in Å.

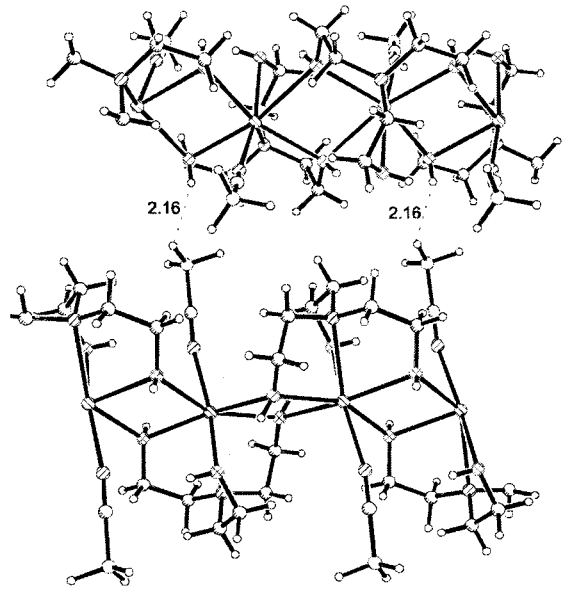

Figure 22. X-ray crystal structure of $NaNCBH_3$·TEA showing the H−H contact distances in Å.

strated that H···H bonds have a role in the formation of dihydrogen η^2-H_2 complexes and the reverse heterolytic splitting of H_2, as well as σ-bond metathesis (Scheme 2). In the solid state, this transformation can be topochemical, transferring the initial order present in the starting dihydrogen-bonded crystal to the newly formed covalent network, thus providing access to novel crystalline materials with desired structures and properties.

Scheme 2

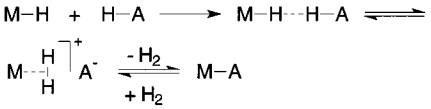

A. Reactivity and Selectivity Control by Dihydrogen Bonding in Solution

The Ir−H_b bond in **33** has been found to be activated by dihydrogen bonding for a number of reactions.[73] Thus, the hydridic and protonic hydrogens H_a and H_b involved in the H···H interaction can interchange relatively easily, whereas the noninteracting H_c is exchanged much more slowly with H_a and H_b. The $\Delta H^{\ddagger}$ for the H_a/H_b exchange was estimated by variable temperature NMR spectroscopy at around 14−16 kcal/mol and found to go down as the R group becomes more electron-withdrawing, consistent with a mechanism involving proton transfer from the OH group to the Ir−H_a bond, to give an η^2-H_2 intermediate complex (Scheme 3). Rotation of the H_2 ligand in this complex and transfer of the proton back to the oxygen completes the exchange. When the reaction was performed in the presence of benzonitrile, the H_2 ligand could be displaced by PhCN, in a rate-limiting step. Alternatively, H_2 elimination from **33** by heating in a sealed tube at 80 °C yielded the chelate complex **33a**, in a σ-bond metathesis reaction. The initial complex **33** could be recovered by exposure to H_2 in CH_2Cl_2 at room temperature, via the isomer **33b** (Scheme 4). Similarly, hydrogen scrambling between H_a and H_b is facilitated by dihydrogen bonding in complexes **34**, apparently via an η^2-H_2 intermediate.[73] H_2 loss at room temperature

Scheme 3

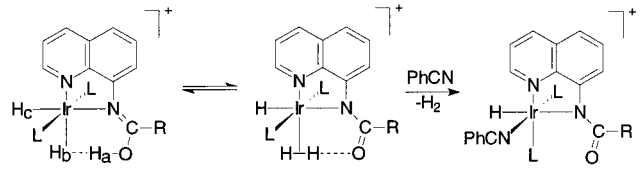

Scheme 4

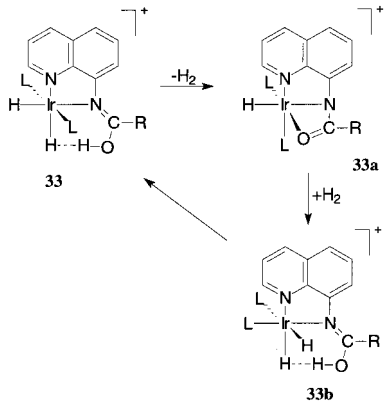

Scheme 5

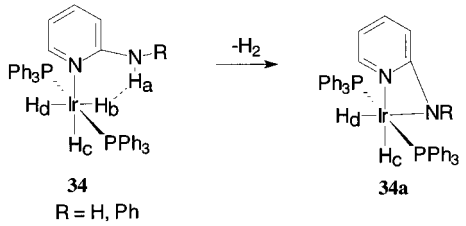

Scheme 6

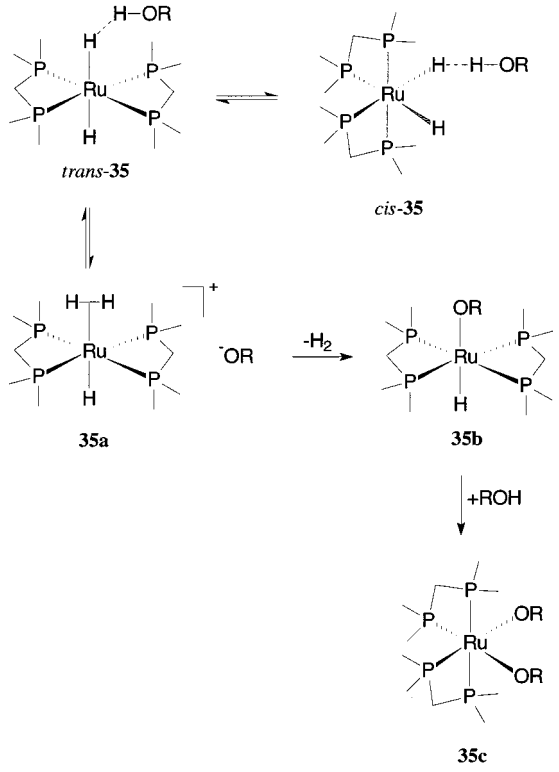

was also observed, with the formation of **34a** in a first-order reaction, with measured activation parameters $\Delta H^{\ddagger}$ and $\Delta S^{\ddagger}$ of 14 ± 2 kcal/mol and −32 ± 6 eu, respectively (Scheme 5). The highly negative activation entropy suggests an associative process with a highly ordered transition state.

The first direct observation of a dynamic equilibrium between a H···H bonded system and an η^2-H_2 complex resulting from proton transfer along a dihydrogen bond was made by Chaudret and coworkers, using NMR spectroscopy.[74] Thus, the ruthenium hydride complex $RuH_2(dppm)_2$·PhOH (**35**) exists as a mixture of dihydrogen-bonded cis and trans isomers in benzene or toluene solutions. The trans isomer is also involved in a dynamic equilibrium with the dihydrogen complex **35a**, which lies 17 kcal/mol lower in enthalpy than **35** (Scheme 6). The entropy change for the same process was found to be −75.8 eu. It was proposed that the reversibility of the process originates in the strong dihydrogen bonding in **35**. In the presence of the more acidic hexafluoro-2-propanol, the corresponding dihydrogen complex **35a** further reacts by H_2 loss, to ultimately give **35c** via **35b**. DFT calculations by Scheiner et al. on a $HOH\cdots H_2Ru(PH_2CH_2PH_2)_2$ model confirmed the higher stability of the dihydrogen complex, which lies 10.7 kcal/mol lower in energy than the dihydrogen-bonded adduct in this case.[75] The activation energy for the proton transfer was estimated around 10 kcal/mol. However, when the stronger proton donor HF was used in the calculations, no F−H···H−Ru adduct could be identified, and the system evolved directly toward a dihydrogen complex, which in this case was found to be 23.8 kcal/mol lower in energy than the separated HF and ruthenium hydride complex.

Scheme 7

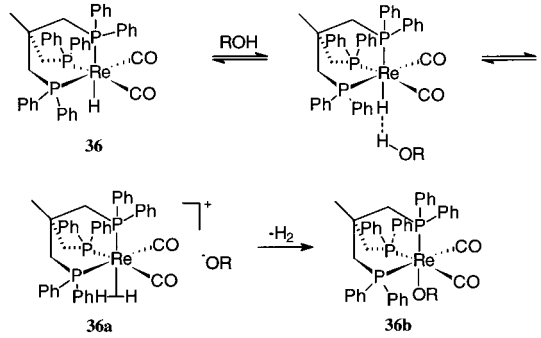

Using in situ IR and NMR spectroscopies, Epstein et al. studied the reversible proton transfer in the dihydrogen-bonded complexes between (triphos)Re-$(CO)_2H$ (**36**) and phenol, tetrafluoroboric acid (HBF_4·OMe_2), chloroacetic acid ($ClCH_2CO_2H$), hexafluoro-2-propanol (HFIP), or perfluoro-2-methyl-2-propanol (PFTB), as proton donors, at 200−260 K (Scheme 7).[76] The η^2-H_2 complexes **36a** were found again to be thermodynamically more stable than their H···H bonded precursors. Higher temperatures induced H_2 loss with the formation of the covalent products **36b**. Similarly, in the case of $H_2Re(CO)(NO)(PMe_3)_2 + CF_3$-COOH, the dihydrogen-bonded complex coexists in equilibrium with the corresponding η^2-H_2 complex.[77] Unfortunately, the instability of the latter relative to H_2 loss precluded the quantitative analysis of this system. The more basic $HW(CO)_2(NO)(PMe_3)_2$ allowed the use of weaker proton donors such as $(CF_3)_2$-CHOH. However, the resulting η^2-H_2 complex was found to be even less stable, rapidly eliminating H_2 with the formation of the corresponding W−OR covalent product. A relatively stable η^2-H_2 complex could be finally obtained using the even more basic $HRu(Cp)(CO)(PCy_3)$. Proton transfer from $(CF_3)_3COH$ was found to be slow, with a barrier of 15 kcal/mol. The resulting dihydrogen complex is stabilized by the formation of η^2-$H_2\cdots A^-$ ionic pairs, whose existence was demonstrated by IR spectroscopy.[77] To model this reaction, Scheiner et al. used the $HRu(Cp)(CO)(PH_3)$ ruthenium hydride model, which was allowed to interact with H_3O^+, CF_3OH, or H_2O, representing strong, moderate, and weak proton donors, respectively.[78] While in the first case spontaneous transfer of proton with the formation of a corresponding hydrated η^2-H_2 complex was observed, the other two weaker acids did not transfer the proton at all, suggesting that the activation barrier for this process is largely determined by the proton donor ability of the acidic partner. The critical role of the proton donor acidity has also been recently recognized by Lau et al., who concluded that strongly acidic condi-

tions give η^2-H_2 complexes, while weakly acidic conditions favor dihydrogen-bonded species.[79]

In the ruthenium polyhydride complex **37**, Chaudret et al. noted a substantial increase of the H−H coupling J_{ab} upon formation of dihydrogen bonding with various proton donors in toluene, which was tentatively explained by the decrease of the electron density on Ru, caused by the partial charge transfer from the metal hydride to the hydrogen bond donor.[80]

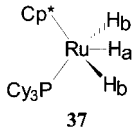

37

When the $CDCl_2F/CDF_3$ (2:1) solvent system was used instead, proton transfer with the formation of the $(Cp^*)(PCy_3)RuH_4$ complex was observed at low temperatures, as a result of the unusual property of the Freon mixture to strongly increase its dielectric constant upon cooling, assisting thus the protonation of **37**.[81] Interestingly, the reactants can be mixed at room temperature, but the proton transfer only occurs when the temperature is sufficiently lowered to induce an adequate increase in the dielectric constant of the solvent. The same behavior was observed in CD_2Cl_2, a solvent which is also known to have a strong temperature-dependent dielectric constant.

According to Lau et al., intramolecular N−H···H−Ru dihydrogen bonds also appear to mediate proton transfer and subsequent formation of N−Ru bonds in **38**, as illustrated in Scheme 8.[82] H/D exchange of both protonic and hydridic hydrogen atoms with D_2O strongly suggest the existence of η^2-H_2 intermediate species in equilibrium with the H···H bonded complexes. H_2 loss with the formation of a Ru−N bonded chelate structure is facile in **38b**, and the reverse Ru−N bond hydrogenolysis can be done at 60 °C under 60 atm (Scheme 8). This system was found to catalyze the reduction of CO_2 to formic acid, although with low yields. The heterolytic splitting of the H_2 ligand is believed to be a crucial step in the proposed mechanism, which is depicted in Scheme 9. The only NMR detectable metal-containing species throughout the reaction is **38**, suggesting that the insertion of CO_2 into the Ru−H bond is the rate-determining step, as also supported by recent theoretical calcula-

Scheme 8

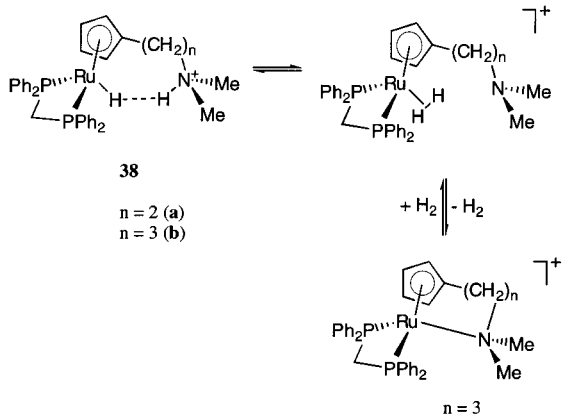

38

n = 2 (**a**)
n = 3 (**b**)

Scheme 9

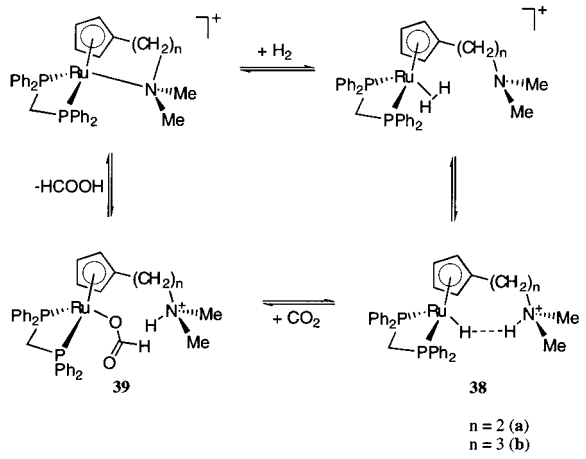

39 **38**

n = 2 (**a**)
n = 3 (**b**)

Scheme 10

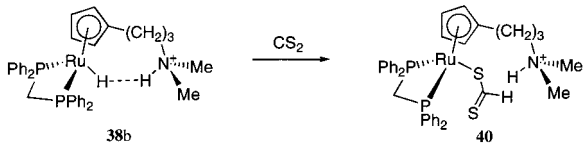

38b **40**

tions on a similar system.[83] While the proposed metal formate intermediate **39** could not be detected, the analogous dithioformate complex **40** was easily prepared from **38b** and excess CS_2 (Scheme 10), and its identity was unambiguously established by IR and NMR spectroscopies.[82]

Hydrogen exchange in the structurally related complex **41** was studied by Chaudret et al. using ^{1}H NMR spectroscopy, and the activation energy for this process was determined to be around 11 kcal/mol.[84] However, extensive DFT calculations suggested that the mechanism for the exchange does not involve any proton transfer within the N−H···H−Ru dihydrogen bond.

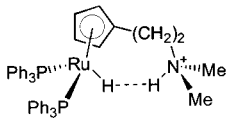

41

A very interesting dihydrogen-bonded system and its hydrogen exchange dynamics have been recently described by Jalón et al.[85] They reported a three-center py_2H···H−Ru intramolecular interaction in **42**, in which fast scrambling between the hydridic and protonic hydrogen atoms occurs most probably via an η^2-H_2 complex intermediate (Scheme 11). An activation energy of about 13.6 kcal/mol was determined for this process, using variable temperature ^{1}H NMR spectroscopy. Moreover, this system proved to be a very active catalyst for D^+/H_2 exchange. Thus, when a solution of **42** in CD_3OD was exposed to a dihydrogen atmosphere at room temperature and 1 atm, more than 90% of H_2 was exchanged for D_2 in about half an hour.

A similar exchange was reported by Morris et al. in the ruthenium polyhydride complex **29b**·[K(1,10-diaza-18-crown-6)] (Scheme 12).[69] Upon exposure to D_2 gas at 1 atm and room temperature for 5 min, the

Scheme 11

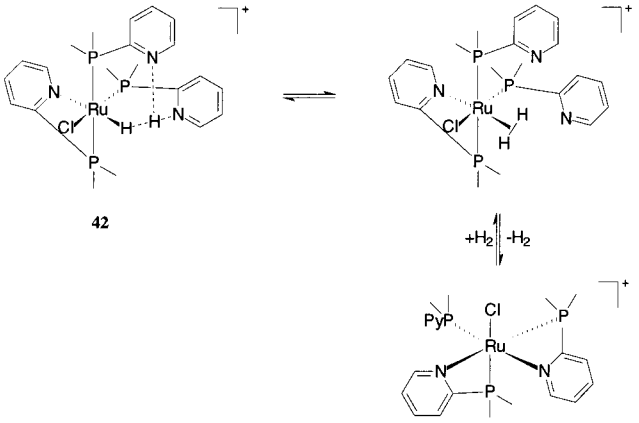

Scheme 12

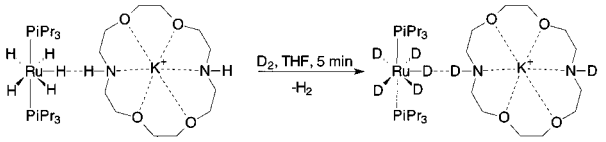

intensities of the NH and RuH ^{1}H NMR (THF-d_8) signals were depleted by 100 and 90%, respectively. For comparison, only 13% decrease in the hydride resonance was observed after 10 days when the much less acidic 18-crown-6 ether was used for complexation, implying efficient activation of the M−H bonds by N−H···H−Ru dihydrogen bonding. The exchange is also significantly slower if the ruthenium hydride is replaced by the less basic analogous osmium hydride (**29a**). While the conjugate acid of **29b**, the known $RuH_2(H_2)_2(^iPr_3)_2$ dihydrogen complex, could reasonably play the role of the intermediate in the exchange process depicted in Scheme 12, its involvement in this transformation was ruled out by control experiments.

Intramolecular N−H···H−Re interactions can affect hydride fluxionality in $ReH_5(PPh_3)_2L$ (L = *N*-acetyl-2-aminopyridine) (**43**).[86] Thus, the free energy of activation for the turnstile rotation involving the H_1, H_4, and H_5 atoms in this complex is 0.7 kcal/mol smaller than for the analogous complex with the NHAc group in the *para* position of the pyridine ring. Stabilization of the transition state by strong N−H···H−Re dihydrogen bonding, which is only possible in the *ortho*-NHAc isomer, seems to be responsible for the observed difference. However, this effect is partly offset by nonbonding repulsive interactions between the two H···H hydrogen atoms, which are forced to approach to 1.49 Å in the transition state, according to theoretical calculations.[87]

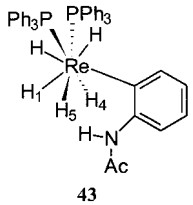

Dihydrogen bonding can have important consequences on the selectivity and stereochemistry of

Scheme 13

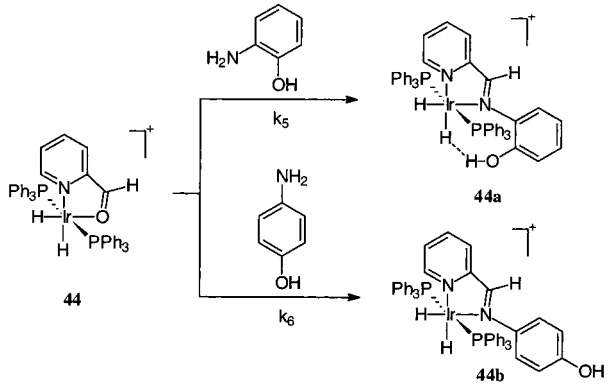

Scheme 14

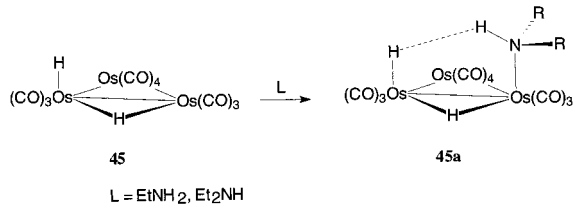

reactions in solution. Thus, the formation of directional and strong H···H interactions can differentially stabilize one particular transition state among two or more possibilities, ultimately controlling the product distribution or stereochemical outcome. An illustration of this concept is the selective imination of the η^1-aldehyde complex **44** with *o*- vs *p*-aminophenol, carried out by Crabtree et al.[88] In a competitive experiment using an equimolecular mixture of 2-aminophenol, 4-aminophenol, and **44**, a 4.2:1 ratio of the resulting products **44a** and **44b** was obtained (Scheme 13), which was calculated to correspond to a k_5/k_6 value of 6. This outcome appears to be the result of O−H···H−Ir dihydrogen bonding stabilization of **44a** (and presumably of the TS leading to it). The two isomers do not interconvert, indicating that the observed product distribution is dictated by kinetic not thermodynamic control. While the observed ratio between the two rate constants is translated into a $\Delta\Delta G^{\ddagger}$ value of 1.1 kcal/mol, the 4.5 kcal/mol estimated H···H interaction energy in **44a** is substantially larger, the difference being apparently offset by the unfavorable chelate ring conformation required for efficient H-bonding in the transition state.

Dihydrogen bonding can also direct the regiochemistry of ligand attachment to transition metal clusters, as demonstrated by Aime and co-workers.[89] Thus, reaction of the electronically unsaturated osmium cluster **45** with $EtNH_2$ or Et_2NH yields exclusively the syn product **45a**, stabilized by an intramolecular N−H···H−Os interaction, which would not be possible in the anti isomer (Scheme 14). Notably, with Et_3N, which lacks the acidic hydrogens required for dihydrogen bond formation, no reaction occurs. The syn isomer is also preponderantly formed when **45** reacts with NH_3. Subsequent treatment with acetaldehyde or acetone in chloroform leads to the exclusive formation of the dihydrogen-bonded imino-derivatives **45b** with a syn configuration (Scheme 15).[90,91] The intramolecular N−H···H−Os interaction is dis-

Scheme 15

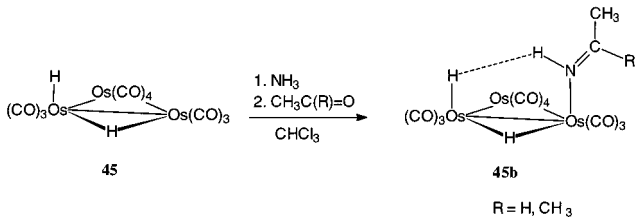

45 45b

R = H, CH_3

rupted in more polar, hydrogen bonding solvents such as methanol or acetone. In this case, the interconversion between the syn and anti isomers was demonstrated by variable temperature NMR spectroscopy, which suggests that the observed regioselectivity is a result of thermodynamic, rather than kinetic control.

The ruthenium hydride **46**, whose crystal structure shows an intramolecular N−H···H−Ru short contact, was found to efficiently catalyze the asymmetric hydrogenation of ketones to chiral alcohols.[92] However, the specific contribution of the H···H interaction to the high enantioselectivity observed in these reductions was not analyzed.

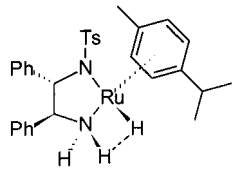

46

Work in our group by Gatling established the ability of O−H···H−B dihydrogen bonds to direct the borohydride reduction of ketones to alcohols.[93] Thus, reductions of 2-hydroxycyclobutanone or 2-hydroxycyclopentanone with tetrabutylammonium borohydride in the non-hydrogen bonding solvents CH_2Cl_2, $ClCH_2CH_2Cl$, or *o*-dichlorobenzene are accelerated about 150 times relative to the reductions of the corresponding unsubstituted cycloalkanones and yield almost exclusively trans diols after workup (Scheme 16). These effects are greatly reduced in the presence of competing hydrogen bonding alcohols or anions such as F^-, Cl^-, or Br^-. Capping of the OH with a trimethylsilyl group also shuts off both the stereodirection and the rate acceleration. AM1 semiempirical calculations predicted a 3.5 kcal/mol preference for the hydride delivery from the OH substituted face of 2-hydroxycyclobutanone (Figure 23), which is in reasonable agreement with the experimental findings, despite the crude level of theory and the absence of counteranions or solvent in the model.

Scheme 16

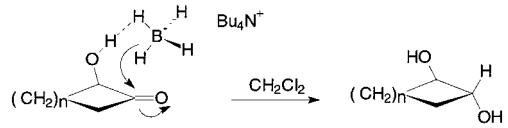

n = 1, 2

B. Reactivity and Selectivity Control by Dihydrogen Bonding in the Solid State

As illustrated in the previous section, many studies regarding the dynamics of dihydrogen-bonded sys-

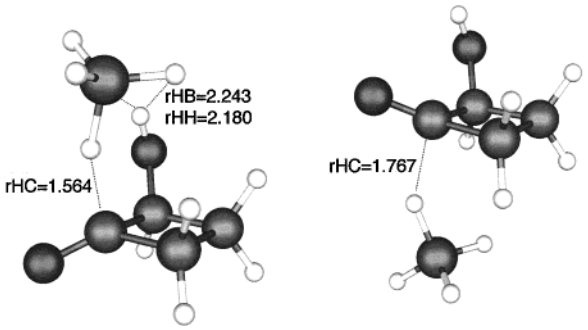

Figure 23. AM1 calculated transition structures for attack of BH_4^- from (left) syn ($\Delta H_f = -81.8$ kcal/mol) and (right) anti ($\Delta H_f = -78.3$ kcal/mol) faces of 2-hydroxy-cyclobutanone, showing salient contact distances (Angstroms).

Scheme 17

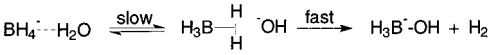

tems in solution have demonstrated that proton transfer from the acidic AH partners to the transition metal hydrides MH, along the H···H bonds, generally leads to η^2-H_2 nonclassical complexes, which subsequently eliminate hydrogen upon heating, with the formation of covalent M−A bonds (Scheme 2). An analogous process appears to occur in the case of the borohydride anion. In aqueous solutions, BH_4^- is very likely dihydrogen-bonded to H_2O, as suggested by the crystal structure of $NaBH_4 \cdot 2H_2O$,[21] as well as theoretical and experimental studies by Epstein et al.[18−20] Under neutral or acidic conditions, borohydrides undergo hydrolysis to boric acid ($B(OH)_3$), for which the established mechanism involves slow proton-transfer resulting in a BH_5 intermediate, followed by fast H_2 loss and B−O bond formation (Scheme 17).[94−97] Activation parameters $\Delta H^{\ddagger}$ and $\Delta S^{\ddagger}$ of 20.6 ± 1 kcal/mol and −22.3 ± 3 eu were measured for the neutral hydrolysis, while under acidic conditions the corresponding values obtained are 8.0 ± 1 kcal/mol and −3 ± 3 eu, respectively.[97] The structure of BH_5, as deduced by theoretical calculations, is best described as an almost planar BH_3 molecule, loosely coordinated by H_2.[98−100] Theoretical work by Elguero et al. indicates that H_2 generation from dihydrogen-bonded borohydrides can also be induced by the internal forces within a crystal.[101]

All these premises, together with the established ability of borohydrides to self-assemble into extended dihydrogen-bonded networks, suggested to us that A−H···H−B dihydrogen bonds could be employed in topochemical assembly of covalent materials.[72] Such weak H···H interactions, in principle, may be used to organize and hold a structure's form while it is more firmly fastened together by A−B bond formation, transferring thus the initial order from the starting crystal to the newly formed covalent frame. This strategy makes dihydrogen bonding a potentially powerful tool for rational assembly of new crystalline covalent materials with controlled structures and properties.

An early example of topochemical control by dihydrogen bonding was the solid-state conversion of cyclotrigallazane (**12**) into nanocrystalline gallium

nitride, reported by Gladfelter and co-workers.[102] Initial loss of H_2 at 150 °C resulted in an amorphous GaN phase, which upon annealing at 600 °C led to the metastable crystalline cubic gallium nitride, as a 1:1 mixture with the thermodynamically favored hexagonal GaN. The crystallization in the cubic system appears to be dictated by the initial crystal packing in **12**, consisting of N−H···H−Ga dihydrogen-bonded chains (Figure 10), which can be considered essentially "hydrogenated" cubic GaN. For comparison, decomposition of cyclotrigallazane in thin films obtained by vapor deposition, a process that presumably disrupts the dihydrogen-bonded network, yields exclusively hexagonal GaN. It is remarkable that despite the huge contraction of the unit cell accompanying the conversion of **12** into cubic GaN, the reaction still maintains partial topochemical character. The price to pay, however, was the initial loss of crystallinity and the consequent requirement for high annealing temperatures to restore it. Although this thermal treatment had no detrimental effect upon the robust GaN, more delicate structures would not tolerate such high temperatures, limiting the general applicability of this approach.

A low temperature procedure for topochemical dihydrogen to covalent bonding transformations would allow the extension of this strategy into the structurally more diverse domain of organic materials. Like many solid-state processes, this reaction includes two threats to the crystalline order: (a) geometry change upon bond reorganization, and (b) gas release within the lattice. Clearly, careful design of the starting dihydrogen-bonded networks is necessary to meet these challenges. Success, however, would mean that the well-developed tools of molecular synthesis could now be applied to the rational construction of crystalline covalent solids with desired structures and functions.

We explored two strategies to address this problem: (a) design of cations to form closed loops in coordination with hydride-bearing anions, in which case the lattice distortion accompanying decomposition would not be cumulative, and (b) selection of globular cations large enough that their close packing determines the lattice parameters, with the hydridic anions fitting into the interstitial holes, in which bond formation via flexible arms would induce minimal change in the unit cell (Scheme 18).[72] A dividend of this latter strategy is that the anticipated looseness of the lattice should allow the released H_2 to diffuse readily through and out of the crystal.

Having intentionally designed it for the purpose, we were delighted to find that crystals of *N*-[2-(6-aminopyridyl)]-acetamidine cyanoborohydride (**47**) comprise two independent examples of closed-loop self-assembly by dihydrogen bonding (Figure 24).[72] However, this compound's decomposition yielded complex mixtures due to the unwanted reduction of the amidine functionality. Additionally, partial liquefaction during the reaction precluded topochemical control, stressing the importance of another design feature for the dihydrogen-bonded systems: the melting temperature, which should be sufficiently high to allow their decomposition to be carried out in the solid.

Scheme 18

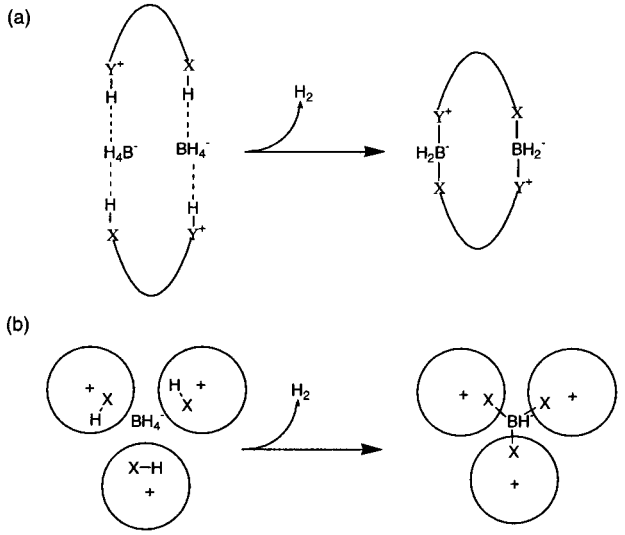

The MBH_3X·TEA (M = Na, Li; X = H, CN; TEA = triethanolamine) complexes **30**−**32** were synthesized as candidates for the globular cations strategy.[71,72] As illustrated in Figure 21, the $NaBH_4$·TEA (**31**) complex self-assembles in two-dimensional hydrogen-bonded layers in the solid state. Its decomposition proved to be topochemical, leading to a polymeric trialkoxyborohydride, in sharp contrast to the $NaBH_4$ and hydride-free polymeric borate disproportionation products obtained from decomposition in solution or melt.[72] While the powder X-ray diffraction pattern of the resulting product indicated the formation of a layered material as expected for this lattice-controlled reaction, its crystallinity was disappointingly poor. With its less basic hydridic sites, the $NaCNBH_3$·TEA complex (**32**) could not be decomposed in the solid-state, losing H_2 only at ca. 100 °C above its melting point, suggesting that as in solution, the relative acidity/basicity of the proton and hydride partners controls the reactivity of the dihydrogen-bonded systems.

Reasoning that the Li^+ cation would complex TEA more strongly, making the OH sites more acidic and hence more reactive, we synthesized the $LiBH_4$·TEA (**30**) complex, which unlike **31**, self-assembles into one-dimensional dihydrogen-bonded ribbons (Figure 20).[71] As predicted, **30** has much greater solid-state reactivity than its Na analogue. Its decomposition is again topochemical, apparently leading to a one-dimensional polymeric trialkoxyborohydride structure (**30a**) (Scheme 19), in direct contrast to decomposition in DMSO solution, which yielded a polymeric

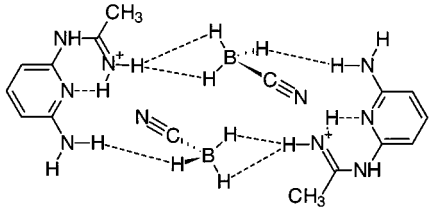

Figure 24. Self-assembly of N-[2-(6-aminopyridyl)]-acetamidine cyanoborohydride in closed-loop dimers.

Scheme 19

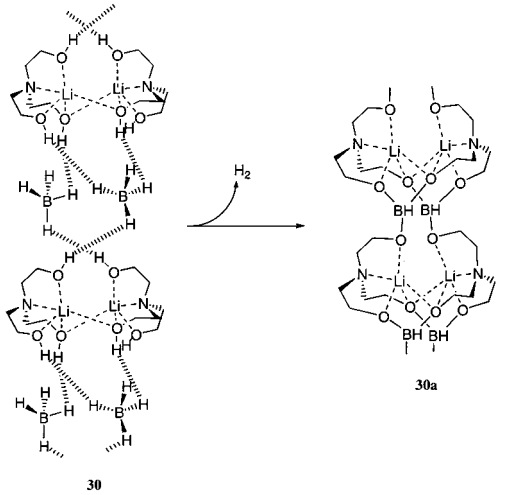

Scheme 20

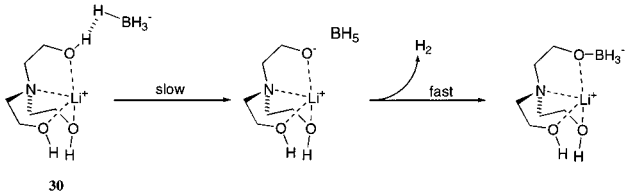

borate and unconverted $LiBH_4$, the disproportionation products. For comparison, no such disproportionation occurs during the solid-state decomposition of **30**, as demonstrated by H/D isotopic labeling experiments.[103] Although more crystalline than the Na system, **30a** is still mostly amorphous, and further annealing at 120 °C induced complete loss of order, pointing out its metastable nature.

The high solid-state reactivity of **30** allowed us to study the mechanism of H_2 loss and covalent bond formation in this dihydrogen-bonded complex both at macroscopic and molecular levels.[103] Using in situ solid-state ^{11}B NMR, optical microscopy, and H/D isotopic labeling studies, we found that, like most solid-state reactions, this decomposition is heterogeneous, with crystallization of the product phase from the parent crystal. Macroscopically, the crystals preserve their original detailed shape, but become opaque as a result of the nucleation and growth of the product nuclei. Kinetic analysis and H/D exchange experiments established that proton transfer between the OH groups of the TEA and the BH_4^- anions, at the reactant/product interface, is the rate-limiting step, with activation parameters $\Delta H^{\ddagger}$ and $\Delta S^{\ddagger}$ of 20.1 ± 2.4 kcal/mol and −16.8 ± 6.2 eu (Scheme 20). These values are comparable with the analogous values found for the aqueous hydrolysis of BH_4^- in neutral water,[97] suggesting similar mechanisms for the solid and solution decompositions.

An example of a dihydrogen-bonded system that combines both the closed loop and the globular cation strategies is the $NaBH_4$·THEC (THEC = *N*,*N*′,*N*″,*N*‴-tetrakis-(2-hydroxyethyl)cyclen) complex (**48**).[104]

This compound's crystal structure consists of D_2 symmetrical dimers, held together by four conventional O−H···O hydrogen bonds, complemented by four orthogonal O−H···H−B proton−hydride interactions (Figure 25). No hydrogen bonds link the dimers, which are packed into two-dimensional layers (Figure 26). Formation of discrete "molecular cages" might thus be expected from solid-state decomposition. Heating **48** in the solid induced complete loss of H_2, as indicated by IR and ^{11}B NMR spectroscopy,

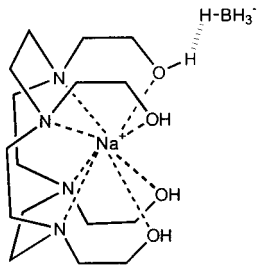

48

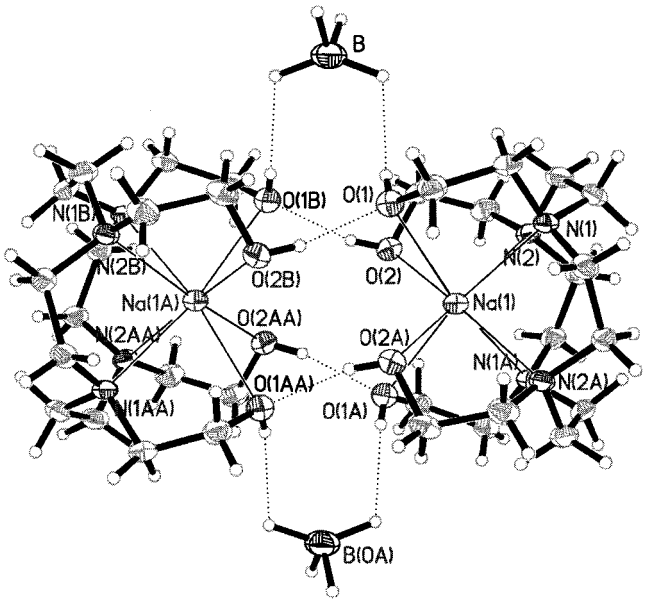

Figure 25. X-ray crystal structure of $NaBH_4$·THEC illustrating the self-assembly in dihydrogen-bonded dimers. Reproduced with permission from ref 104. Copyright 1999 Wiley-VCH.

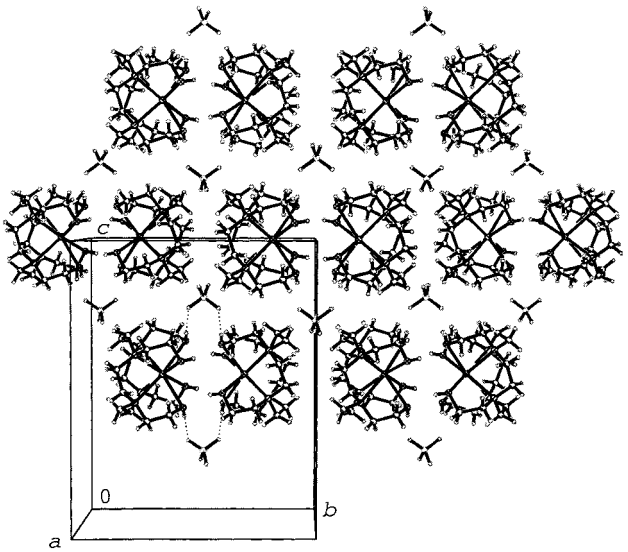

Figure 26. Crystal packing in $NaBH_4$·THEC. Reproduced with permission from ref 104. Copyright 1999 Wiley-VCH.

as well as TGA, with the formation of a highly crystalline product. Remarkably, the decomposition is crystallographically homogeneous, as demonstrated by polarizing microscopy and powder X-ray diffraction, which indicates a 9% shrinkage of the unit cell during this crystal-to-crystal process. However, despite our sustained efforts, the detailed structure of the resulting crystalline product has remained elusive to date, due to deterioration of the single crystals' quality and insolubility in common solvents. Nevertheless, this study is the first example to demonstrate that judicious engineering of dihydrogen-bonded crystals permits transfer of crystallinity to the covalent products resulting from their solid-state decomposition. The implication is that this strategy may ultimately lead to low temperature, rational construction of extended crystalline covalent solids, a class of compounds generally accessible only by empirical methods or serendipitous discoveries.

V. Conclusions and Future Prospects

Dihydrogen bonding is now a well-established interaction between hydridic hydrogens, or more accurately σ-bonding electron pairs of M−H bonds (M = Al, B, Ga, Ir, Mo, Mn, Os, Re, Ru, W) and traditional X−H proton donors (X = F, O, N, C). Geometrically, it is usually characterized by short H···H contact distances (typically 1.7−2.2 Å) and strongly bent XH···H−M angles (typically 90−135°). With interaction energies generally situated between 1 and 7 kcal/mol, dihydrogen bonds are comparable with moderately strong conventional hydrogen bonds. Their nature is mostly electrostatic, although a weak covalent contribution may be found sometimes.

Dihydrogen bonds can control reactivity and selectivity in solution. Hydrogen exchange, σ-bond metathesis, ligand attachment to transition metal clusters, and hydride reduction are just a few examples of processes that can be markedly influenced by H···H interactions, and more applications of dihydrogen bonding in catalysis are soon to be expected.

In the solid state, dihydrogen bonds can exert considerable influence on crystal packing, potentially serving as control elements in crystal engineering. Once sufficiently reliable H···H motifs are found, these interactions may become powerful tools for supramolecular synthesis. However, a systematic understanding of the factors governing the three-dimensional arrangement of dihydrogen-bonded molecular crystals will be needed before H···H bonds can effectively be used to assemble materials with targeted structures and properties. The unique ability of dihydrogen bonds to lose H_2 in the solid state, trading the weak H···H interactions for strong covalent bonds, promises new routes to the rational assembly of ordered, extended covalent materials. This recently articulated strategy may soon become a well-traveled bridge connecting the fields of supramolecular and macromolecular chemistries.

VI. Acknowledgments

This work was supported by the MSU Center for Fundamental Materials Research. The support from MSU's Harold Hart endowed fellowship (2000) is also gratefully acknowledged by R.C.

VII. References

(1) Jeffrey, G. A. *An Introduction to Hydrogen Bonding*; Oxford University Press: Oxford, 1997.
(2) Jeffrey, G. A.; Saenger, W. *Hydrogen Bonding in Biological Structures*; Springer-Verlag: Berlin, 1991.
(3) Calhorda, M. J. *Chem. Commun.* **2000**, 801.
(4) Shubina, E. S.; Belkova, N. V.; Epstein, L. M. *J. Organomet. Chem.* **1997**, *536−537*, 17.
(5) Crabtree, R. H.; Siegbahn, P. E. M.; Eisenstein, O.; Rheingold, A. L.; Koetzle, T. F. *Acc. Chem. Res.* **1996**, *29*, 348.
(6) Crabtree, R. H. *J. Organomet. Chem.* **1998**, *577*, 111.
(7) Alkorta, I.; Rozas, I.; Elguero, J. *Chem. Soc. Rev.* **1998**, *27*, 163.
(8) Crabtree, R. H. *Science* **1998**, *282*, 2000.
(9) Crabtree, R. H.; Eisenstein, O.; Sini, G.; Peris, E. *J. Organomet. Chem.* **1998**, *567*, 7.
(10) Kelly, P.; Loza, M. *Chem. Britain* **1999**, *35*, 26.
(11) Zachariasen, W. H.; Mooney, R. C. L. *J. Chem. Phys.* **1934**, *2*, 34.
(12) We have recently redetermined the crystal structure of ammonium hypophosphite at higher resolution, which allowed us to locate the H atoms and thus probe the existence of dihydrogen bonding. However, we found no close H···H contacts in this salt. Stein, R.; Custelcean, R.; Jackson, J. E., manuscript in preparation.
(13) Burg, A. B. *Inorg. Chem.* **1964**, *3*, 1325.
(14) Titov, L. V.; Makarova, M. D.; Rosolovskii, V. Y. *Dokl. Akad. Nauk* **1968**, *180*, 381.
(15) Brown, M. P.; Heseltine, R. W. *Chem. Commun.* **1968**, 1551.
(16) Brown, M. P.; Heseltine, R. W.; Smith, P. A.; Walker, P. J. *J. Chem. Soc. A* **1970**, 410.
(17) Brown, M. P.; Walker, P. J. *Spectrochim. Acta* **1974**, *30A*, 1125.
(18) Shubina, E. S.; Bachmutova, E. V.; Saitkulova, L. N.; Epstein, L. M. *Mendeleev Commun.* **1997**, 83.
(19) Epstein, L. M.; Shubina, E. S.; Bakhmutova, E. V.; Saitkulova, L. N.; Bakhmutov, V. I.; Chistyakov, A. L.; Stankevich, I. V. *Inorg. Chem.* **1998**, *37*, 3013.
(20) Shubina, E. S.; Belkova, N. V.; Bakhmutova, E. V.; Saitkulova, L. N.; Ionidis, A. V.; Epstein, L. M. *Russ. Chem. Bull.* **1998**, *47*, 817.
(21) Jackson, J. E.; Huang, R.; Eckert, J.; Sharma, M.; Argyriou, D.; Sheldon, R., manuscript in preparation.
(22) Richardson, T. B.; de Gala, S.; Crabtree, R. H.; Siegbhan, P. E. M. *J. Am. Chem. Soc.* **1995**, *117*, 12875.
(23) Cramer, C. J.; Gladfelter, W. L. *Inorg. Chem.* **1997**, *36*, 5358.
(24) Klooster, W. T.; Koetzle, T. F.; Siegbahn, P. E. M.; Richardson, T. B.; Crabtree, R. H. *J. Am. Chem. Soc.* **1999**, *121*, 6337.
(25) Popelier, P. L. A. *J. Phys. Chem. A* **1998**, *102*, 1873.
(26) Nöth, H.; Thomas, S. *Eur. J. Inorg. Chem.* **1999**, 1373.
(27) Zottola, M. A.; Pedersen, L. G.; Singh, P.; Shaw, B. R. *Modeling the Hydrogen Bond*; Smith, D. A., Ed.; ACS Symposium Series: American Chemical Society, Washington, DC, 1994; Vol. 569, pp 277−285.
(28) Singh, P.; Zottola, M.; Huang, S.; Shaw, B. R.; Pedersen, L. G. *Acta Crystallogr.* **1996**, *C52*, 693.
(29) Padilla-Martiñez, I. R.; Rosalez-Hoz, M. de J.; Tlahuext, H.; Camacho-Camacho, C.; Ariza-Castolo, A.; Contreras, R. *Chem. Ber.* **1996**, *129*, 441.
(30) This number was obtained using the value of 1.45 Å as the van der Waals radius for the hydridic hydrogen.
(31) Flores-Parra, A.; Sánchez-Ruiz, S. A.; Guadarrama, C.; Nöth, H.; Contreras, R. *Eur. J. Inorg. Chem.* **1999**, 2069.
(32) Atwood, J. L.; Koutsantonis, G. A.; Lee, F.-C.; Raston, C. L. *Chem. Commun.* **1994**, 91.
(33) Campbell, J. P.; Hwang, J. W.; Young, V. G.; Von Dreele, R. B.; Cramer, C. J.; Gladfelter, W. L. *J. Am. Chem. Soc.* **1998**, *120*, 521.
(34) Liu, Q.; Hoffmann, R. *J. Am. Chem. Soc.* **1995**, *117*, 10108.
(35) Alkorta, I.; Elguero, J.; Foces-Foces, C. *Chem. Commun.* **1996**, 1633.
(36) Remko, M. *Mol. Phys.* **1998**, *94*, 839.
(37) Kulkarni, S. A. *J. Phys. Chem. A* **1998**, *102*, 7704.
(38) Kulkarni, S. A.; Srivastava, A. K. *J. Phys. Chem. A* **1999**, *103*, 2836.
(39) Lundell, J.; Pettersson, M. *Phys. Chem. Chem. Phys.* **1999**, *1*, 1601.
(40) Grabowski, S. J. *Chem. Phys. Lett.* **1999**, *312* (5−6), 542.
(41) Grabowski, S. J. *J. Phys. Chem.* **2000**, *104*, 5551.
(42) Milstein, D.; Calabrese, J. C.; Williams, I. D. *J. Am. Chem. Soc.* **1986**, *108*, 6387.
(43) Stevens, R. C.; Bau, R.; Milstein, D.; Blum, O.; Koetzle, T. F. *J. Chem. Soc., Dalton Trans.* **1990**, 1429.
(44) Feracin, S.; Bürgi, T.; Bakhmutov, V. I.; Eremenko, I.; Vorontsov, E. V.; Vimenits, A. B.; Berke, H. *Organometallics* **1994**, *13*, 4194.

(45) Lee, J. C.; Rheingold, A. L.; Muller, B.; Pregosin, P. S.; Crabtree, R. H. *Chem. Commun.* **1994**, 1021.
(46) Peris, E.; Lee, J. C.; Rambo, J. R., Eisenstein, O.; Crabtree, R. H. *J. Am. Chem. Soc.* **1995**, *117*, 3485.
(47) Lough, A. J.; Park, S.; Ramachandran, R.; Morris, R. H. *J. Am. Chem. Soc.* **1994**, *116*, 8356.
(48) Park, S.; Ramachandran, R.; Lough, A. J.; Morris, R. H. *Chem. Commun.* **1994**, 2201.
(49) Park, S.; Lough, A. J.; Morris, R. H. *Inorg. Chem.* **1996**, *35*, 3001.
(50) Wessel, J.; Lee, J. C.; Peris, E.; Yap, G. P. A.; Fortin, J. B.; Ricci, J. S.; Sini, G.; Albinati, A.; Koetzle, T. F.; Eisenstein, O.; Rheingold, A. L.; Crabtree, R. H. *Angew. Chem., Int. Ed. Engl.* **1995**, *34*, 2507.
(51) Patel, B. P.; Wessel, J.; Yao, W.; Lee, J. C. Jr.; Peris, E.; Koetzle, T. F.; Yap, G. P. A.; Fortin, J. B.; Ricci, J. S.; Sini, G.; Albinati, A.; Eisenstein, O.; Rheingold, A. L.; Crabtree, R. H. *New J. Chem.* **1997**, *21*, 413.
(52) Sini, G.; Eisenstein, O.; Yao, W.; Crabtree, R. H. *Inorg. Chim. Acta* **1998**, *280*, 26.
(53) Patel, B. P.; Yao, W.; Yap, G. P. A.; Rheingold, A. L.; Crabtree, R. H. *Chem. Commun.* **1996**, 991.
(54) Peris, E.; Wessel, J.; Patel, B. P.; Crabtree, R. H. *Chem. Commun.* **1995**, 2175.
(55) Desmurs, P.; Kavallieratos, K.; Yao, W.; Crabtree, R. H. *New J. Chem.* **1999**, *23*, 1111.
(56) Shubina, E. S.; Belkova, N. V.; Krylov, A. N.; Vorontsov, E. V.; Epstein, L. M.; Gusev, D. G.; Niedermann, M.; Berke, H. *J. Am. Chem. Soc.* **1996**, *118*, 1105.
(57) Belkova, N. V.; Shubina, E. S.; Ionidis, A. V.; Epstein, L. M.; Jacobsen, H.; Messmer, A.; Berke, H. *Inorg. Chem.* **1997**, *36*, 1522.
(58) Messmer, A.; Jacobsen, H.; Berke, H. *Chem. Eur. J.* **1999**, *5*, 3341.
(59) Scheiner, S.; Orlova, G. *J. Phys. Chem. A* **1998**, *102*, 260.
(60) Richardson, T. B.; Koetzle, T. F.; Crabtree, R. H. *Inorg. Chim. Acta* **1996**, *250*, 69.
(61) Xu, W.; Lough, A. J.; Morris, R. H. *Can. J. Chem.* **1997**, *75*, 475.
(62) Huang, L.-Y.; Aulwurm, U. R.; Heinemann, F. W.; Knoch, F.; Kisch, H. *Chem. Eur. J.* **1998**, *4*, 1641.
(63) Junk, P. C.; Steed, J. W. *J. Organomet. Chem.* **1999**, *587*, 191.
(64) Braga, D.; De Leonardis, P.; Grepioni, F.; Tedesco, E.; Calhorda, M. J. *Inorg. Chem.* **1998**, *37*, 3337.
(65) Custelcean, R.; Jackson, J. E., unpublished results.
(66) Abramov, Y. A.; Brammer, L.; Klooster, W. T.; Bullock, R. M. *Inorg. Chem.* **1998**, *37*, 6317.
(67) Gusev, D. G.; Lough, A. J.; Morris, R. H. *J. Am. Chem. Soc.* **1998**, *120*, 13138.
(68) Abdur-Rashid, K.; Gusev, D. G.; Landau, S. E.; Lough, A. J.; Morris, R. H. *J. Am. Chem. Soc.* **1998**, *120*, 11826.
(69) Abdur-Rashid, K.; Gusev, D. G.; Lough, A. J.; Morris, R. H. *Organometallics* **2000**, *19*, 834.
(70) Jackson, J. E.; Bass, S.; Huang, R., unpublished results.
(71) Custelcean, R.; Jackson, J. E. *Angew. Chem., Int. Ed. Engl.* **1999**, *38*, 1661.
(72) Custelcean, R.; Jackson, J. E. *J. Am. Chem. Soc.* **1998**, *120*, 12935.
(73) Lee, J. C.; Peris, E.; Rheingold, A. L.; Crabtree, R. H. *J. Am. Chem. Soc.* **1994**, *116*, 11014.
(74) Ayllón, J. A.; Gervaux, C.; Sabo-Etienne, S.; Chaudret, B. *Organometallics* **1997**, *16*, 2000.
(75) Orlova, G.; Scheiner, S.; Kar, T. *J. Phys. Chem. A* **1999**, *103*, 514.
(76) Shubina, E. S.; Belkova, N. V.; Bakhmutova, E. V.; Vorontsov, E. V.; Bakhmutov, V. I.; Ionidis, A. V.; Bianchini, C.; Marvelli, L.; Peruzzini, M.; Epstein, L. M. *Inorg. Chim. Acta* **1998**, *280*, 302.
(77) Epstein, L. M.; Shubina, E. S. *Ber. Bunsen-Ges. Phys. Chem.* **1998**, *102*, 359.
(78) Orlova, G.; Scheiner, S. *J. Phys. Chem. A* **1998**, *102*, 4813.
(79) Chu, H. S.; Xu, Z.; Ng, S. M.; Lau, C. P.; Lin, Z. *Eur. J. Inorg. Chem.* **2000**, 993.
(80) Ayllón, J. A.; Sabo-Etienne, S.; Chaudret, B.; Ulrich, S.; Limbach, H.-H. *Inorg. Chim. Acta* **1997**, *259*, 1.
(81) Gründemann, S.; Ulrich, S.; Limbach, H.-H.; Golubev, N. S.; Denisov, G. S.; Epstein, L. M.; Sabo-Etienne, S.; Chaudret, B. *Inorg. Chem.* **1999**, *38*, 2550.
(82) Chu, H. S.; Lau, C. P.; Wong, K. Y.; Wong, W. T. *Organometallics* **1998**, *17*, 2768.
(83) Musashi, Y.; Sakaki, S. *J. Am. Chem. Soc.* **2000**, *122*, 3867.
(84) Ayllón, J. A.; Sayers, S. F.; Sabo-Etienne, S.; Donnadieu, B.; Chaudret, B. *Organometallics* **1999**, *18*, 3981.
(85) Caballero, A.; Jalón, F. A.; Manzano, B. R. *Chem. Commun.* **1998**, 1879.
(86) Patel, B. P.; Kavallieratos, K.; Crabtree, R. H. *J. Organomet. Chem.* **1997**, *528*, 205.
(87) Bosque, R.; Maseras, F.; Eisenstein, O.; Patel, B. P.; Yao, W.; Crabtree, R. H. *Inorg. Chem.* **1997**, *36*, 5505.
(88) Yao, W.; Crabtree, R. H. *Inorg. Chem.* **1996**, *35*, 3007.
(89) Aime, S.; Gobetto, R.; Valls, E. *Organometallics* **1997**, *16*, 5140.
(90) Aime, S.; Férriz, M.; Gobetto, R.; Valls, E. *Organometallics* **1999**, *18*, 2030.
(91) Aime, S.; Férriz, M.; Gobetto, R.; Valls, E. *Organometallics* **2000**, *19*, 707.
(92) Haack, K.-J.; Hashiguchi, S.; Fujii, A.; Ikariya, T.; Noyori, R. *Angew. Chem., Int. Ed. Engl.* **1997**, *36*, 285.
(93) Gatling, S. C.; Jackson, J. E. *J. Am. Chem. Soc.* **1999**, *121*, 8655.
(94) Davis, R. E. *J. Am. Chem. Soc.* **1962**, *84*, 892.
(95) Kreevoy, M. M.; Hutchins, J. E. C. *J. Am. Chem. Soc.* **1969**, *91*, 4329.
(96) Pepperberg, I. M.; Halgren, T. A.; Lipscomb, W. N. *J. Am. Chem. Soc.* **1976**, *98*, 3442.
(97) Mesmer, R. E.; Jolly, W. L. *Inorg. Chem.* **1962**, *1*, 608.
(98) Schreiner, P. R.; Schaefer, H. F.; Schleyer, P. v. R. *J. Chem. Phys.* **1994**, *101*, 7625.
(99) Watts, J. D.; Bartlett, R. J. *J. Am. Chem. Soc.* **1995**, *117*, 825.
(100) Custelcean, R. *J. Mol. Struct. Theochem.* **2000**, *505*, 95.
(101) Rozas, I.; Alkorta, I.; Elguero, J. *Chem. Phys. Lett.* **1997**, *275*, 423.
(102) Hwang, J.-W.; Campbell, J. P.; Kozubowski, J.; Hanson, S. A.; Evans, J. F.; Gladfelter, W. L. *Chem. Mater.* **1995**, *7*, 517.
(103) Custelcean, R.; Jackson, J. E. *J. Am. Chem. Soc.* **2000**, *122*, 5251.
(104) Custelcean, R.; Vlassa, M.; Jackson, J. E. *Angew. Chem., Int. Ed.* **2000**, *39*, 3299.

CR000021B